Digital Holographic Microscopy Techniques for Applications in Cytometry and Histology

Björn Kemper

1.6.2021

Biomedical Technology Center of the Medical Faculty
University of Muenster
Mendelstr. 17, D-48149 Muenster, Germany

- **Digital holographic microscopy (DHM)**
  - **Principles**
  - **Setups**
- **Extraction of biophysical parameters (illustrated by selected applications)**
  - **Adherent cell cultures**
  - **Suspended cells**
  - **Histological tissues**

BIOMED TECH
BioMedizinisches Technologiezentrum

Quantitative phase imaging with digital holographic microscopy (DHM)

Digital Holographic Microscopy

Features

- non-contact / non-destructive
- label-free
- full-field (no scanning)
- on-line (t_{exp}< 1 ms)
- multi-focus, autofocus, subsequent numerical refocusing
- resolution:
  - axial < 3 nm (depends on sample/setup)
  - lateral < 300 nm (diffraction limited)
  - ≈ 70 nm (synthetic aperture microscopy ➔ 3D nanoscopy)

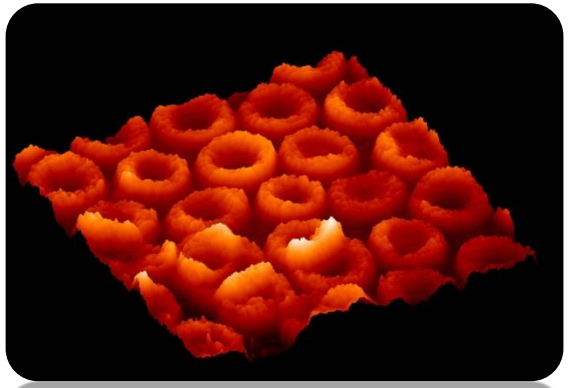

quantitative phase imaging (QPI)

Applications of quantitative phase imaging

Non-destructive testing

- surface metrology / topography measurements
- deformation analysis
- monitoring of photo disruption

Quantitative imaging of cells and tissue

- morphology analysis ➔ reaction on drugs and toxins, cellular mechanics
- online growth analysis ➔ proliferation monitoring
- 2D, 3D cell tracking ➔ migration, motility
- refractive index ➔ intracellular (protein) concentrations, dry mass, label-free tomography, (optical) density of tissue sections

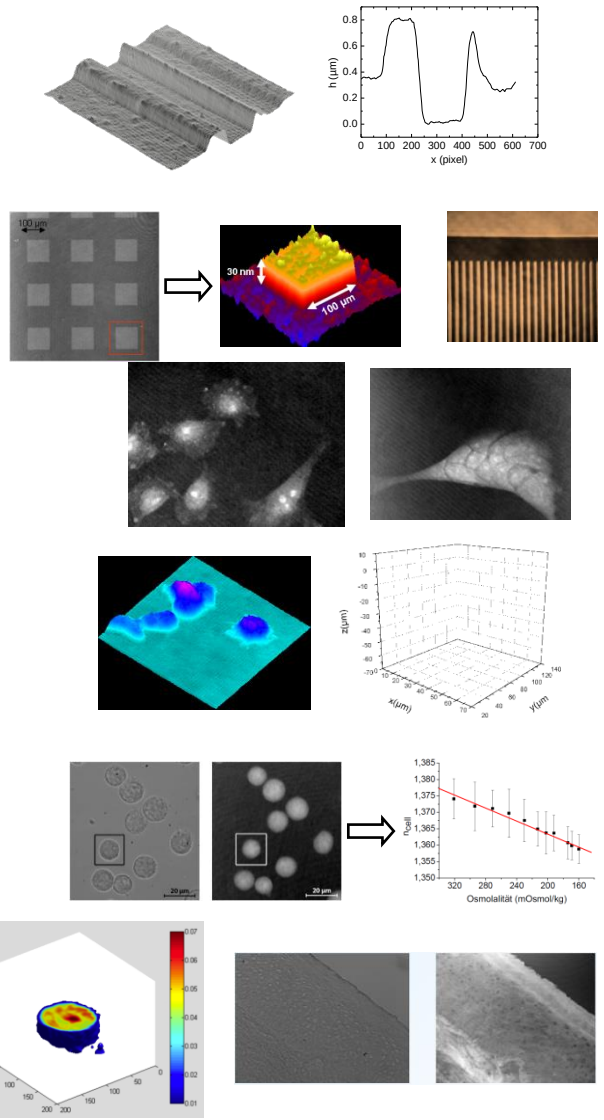

Recent review publications:
Y. K. Park, C. Depeursinge, G. Popescu, *Nat. Photon.* 12, 578-589 (2018).
B. Kemper et. al, Bioanalytical Reviews (2019), Ed.: J. Wegener, BIOREV (2019) 2: 219–272, Springer Nature)
T. Cacace, V. Bianco, P. Ferraro, Opt. Lasers Eng., 135. 106188 (2020)
…

Digital Holographic Microscopy (DHM)

Lens less setup

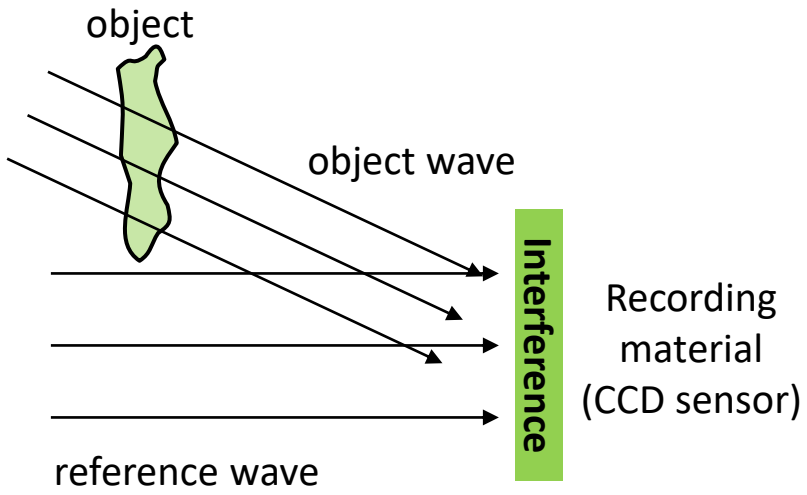

E. N. Leith, and J. Upatnieks, J. Opt. Soc. Am. 52, 1123-1130 (1962).

Utilization of optical imaging systems

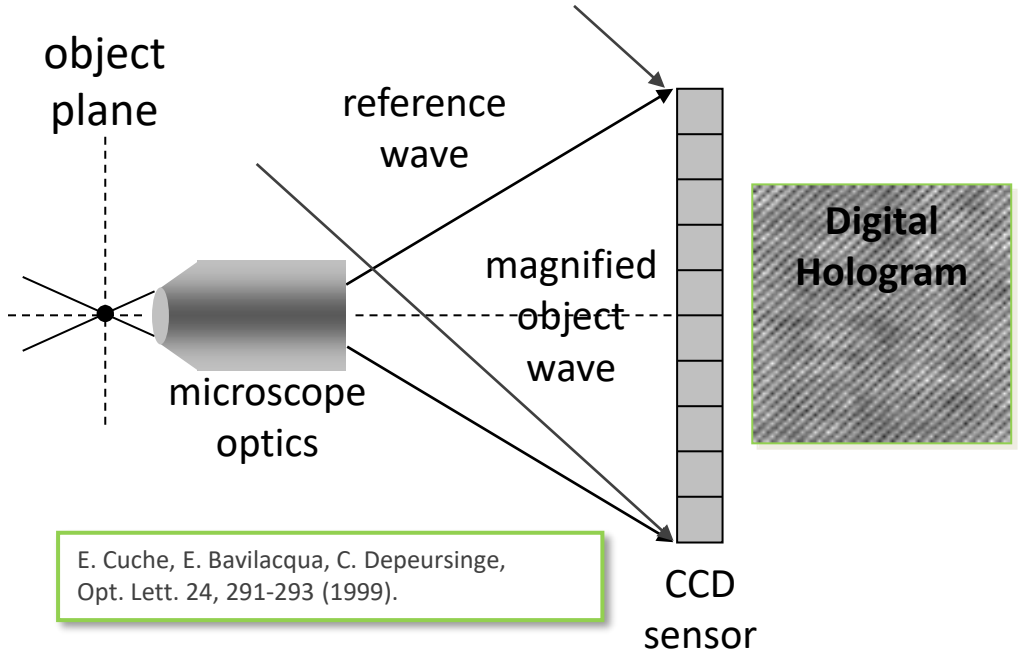

E. Cuche, E. Bavilacqua, C. Depeursinge, Opt. Lett. 24, 291-293 (1999).

following Gabor, Nature161, 777–778 (1948) Nobel Prize in Physics (1971) shortly after the invention of the laser, Maiman, Nature,187, 493–494 (1960)

Modular DHM for quantitative phase imaging of living cell cultures and *ex vivo* tissues

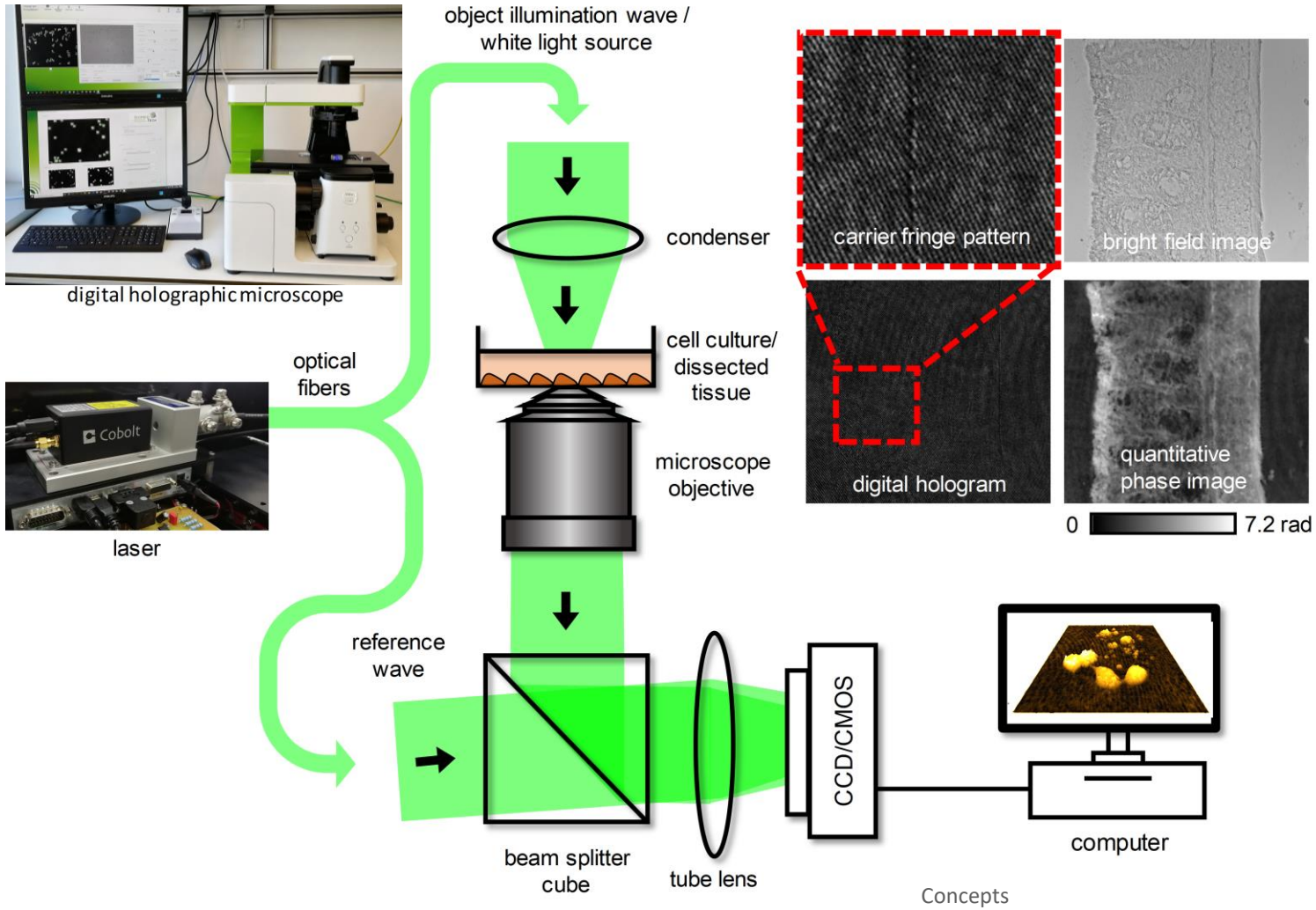

B. Kemper, Europhotonics Winter 2019 issue, 20-23 (2019).

Concepts
B. Kemper, et al. , Proc. SPIE 6191, 61910T (2006).
P. Lenz, et al., J. Vis. Exp. 115, e54460 (2016).

Recording and numerical reconstruction of digital off-axis holograms

BIOMED TECH
BioMedizinisches Technologiezentrum

Living cell in a petri dish (phase object)

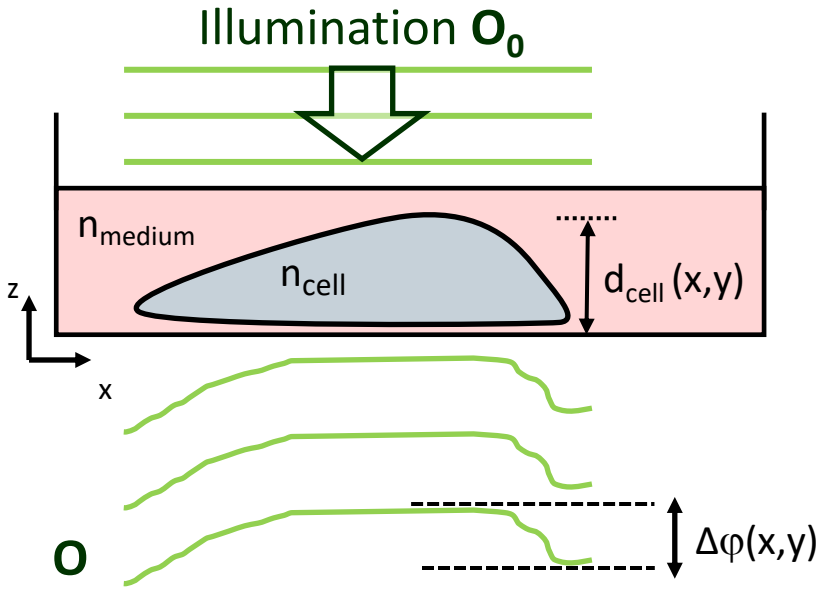

$$\Delta\varphi = \frac{2\pi}{\lambda} d_{cell} \cdot (n_{cell} - n_{medium})$$

digital off- axis hologram (red blood cells)

spatial carrier fringes

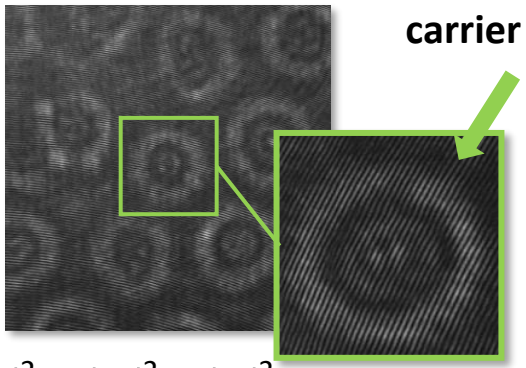

$$I_H \propto |O+R|^2 = |O|^2 + |R|^2 + O^*R + R^*O$$

numerical propagation of *O* (optional)

O(hologram plane) $\rightarrow O'$(image plane)

$\Delta\varphi = \arctan(\mathrm{Im}(O')/\mathrm{Re}(O'))$ (mod2π)

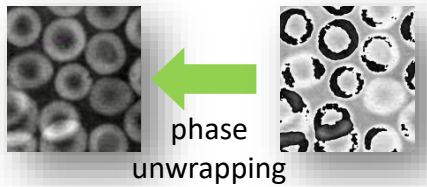

phase unwrapping

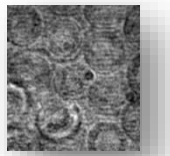

$|O'|$

quantitative phase image

amplitude image

Carl et al., *Appl. Opt*. 43, 6536-6544 (2004)
Kemper et al., *J. Biomed. Opt*. 11 034005 (2006)
Langehanenberg et al., *Appl. Opt*. 47, D176-D182 (2008)
Kemper et al, *Appl. Opt*. 47, A52-A61 (2008)
Min et al., *Opt. Lett.* 42, 227-230 (2017).

Fourier transformation-based evaluation of off-axis holograms with simultaneous compensation of spherical aberrations

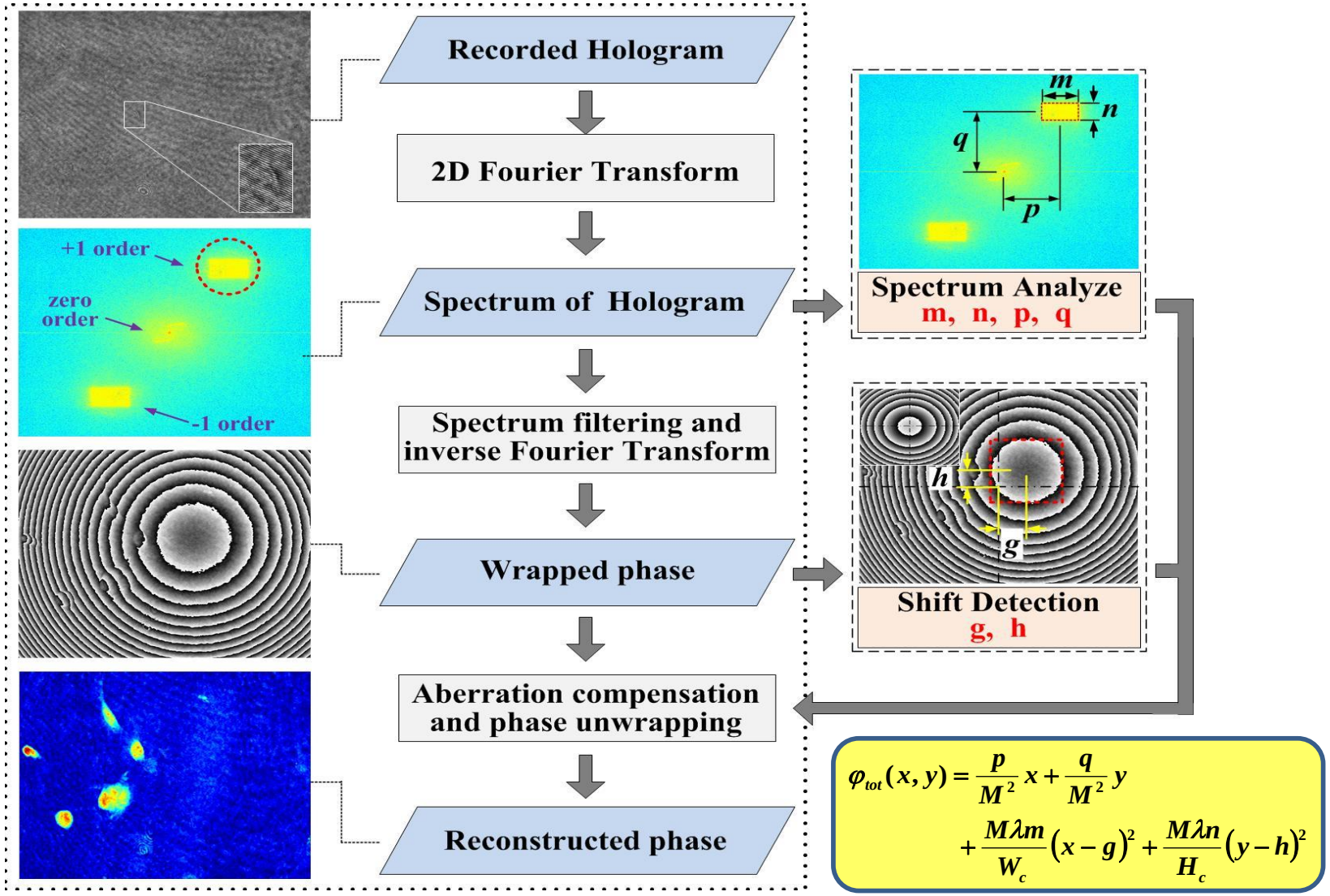

Min et al., *Opt. Lett.* 42, 227-230 (2017).

Modular DHM @ BMTZ

BioMed TECH
BioMedizinisches Technologiezentrum

Flexible “general purpose” system

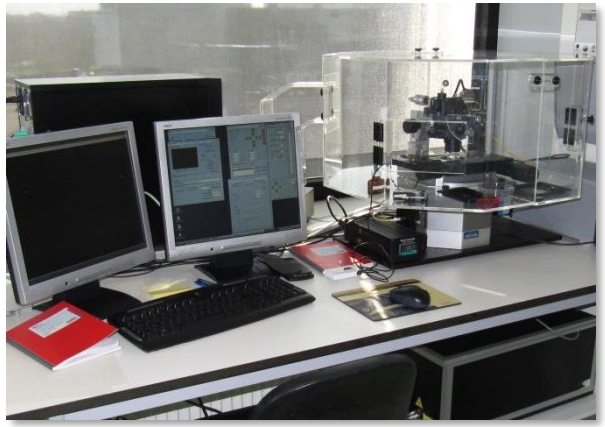

Automated live cell imaging

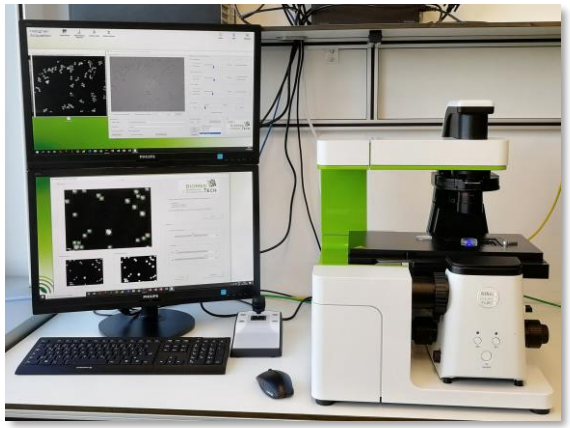

Multi-spectral DHM (450-1700nm)

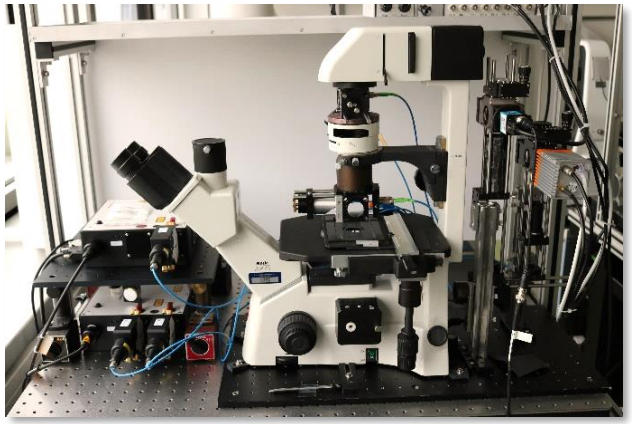

Physiological Environment: CO_2 atmosphere, T = 37 ° C

Software

reconstruction

segmentation

parameter retrieval
(refractive index,
volume, dry mass,…)

cell tracking

Modular DHM @ BMTZ

BioMed BioMedizinisches Technologiezentrum TECH

Flexible “general purpose” system

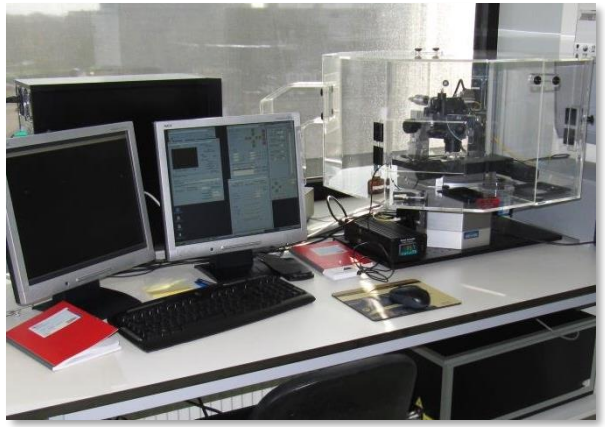

automated live cell imaging

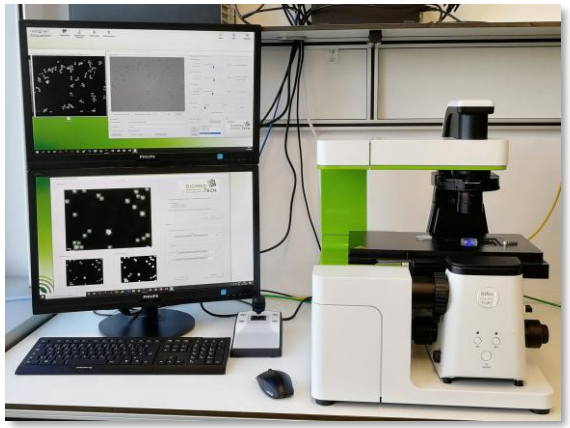

Multi-spectral DHM (450-1700nm)

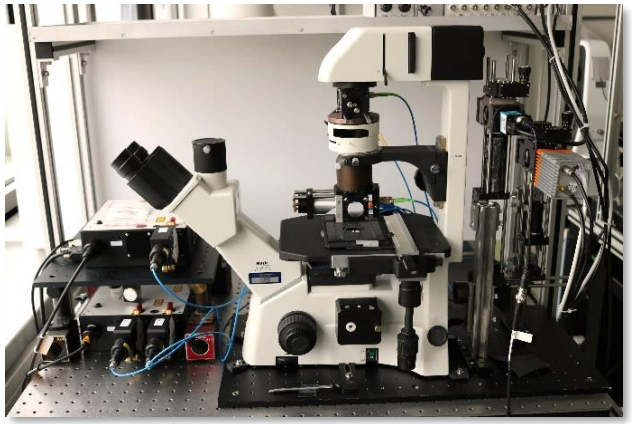

Physiological Environment: CO_2 atmosphere, T = 37 ° C

suspended cells

phenotyping,
cell culture quality control

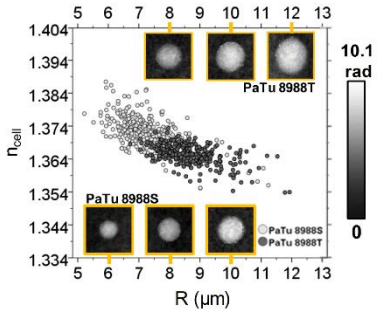

adherend cells

dynamic morphology imaging

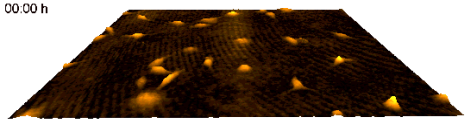

automated cell tracking

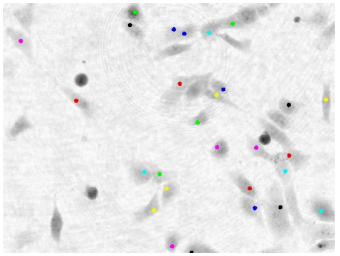

tissue slices

quantification of inflammation
mediated tissue sections

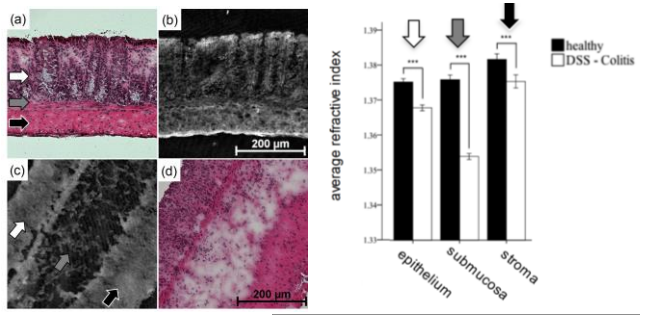

Modular DHM @ BMTZ

BioMed BioMedizinisches Technologiezentrum TECH

Flexible “general purpose” system

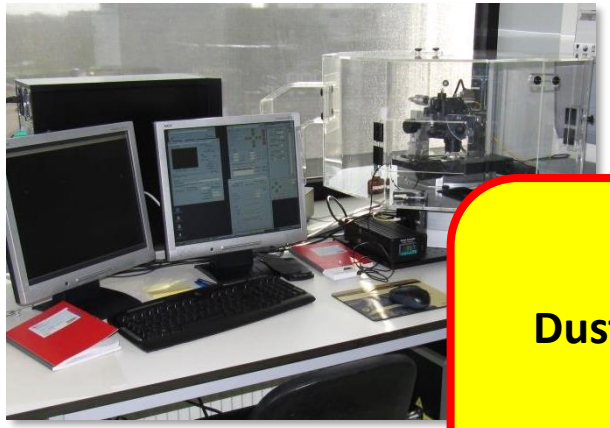

automated live cell imaging

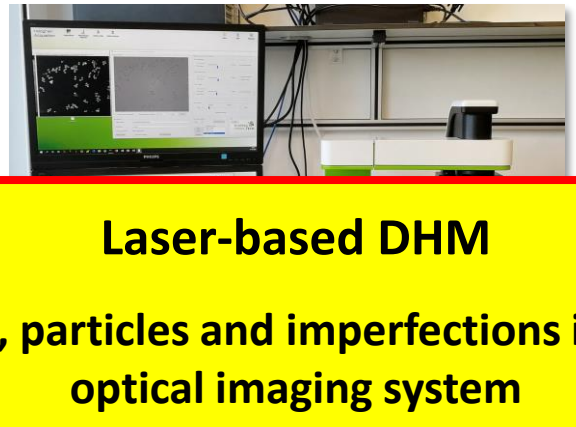

Multi-spectral DHM (450-1700nm)

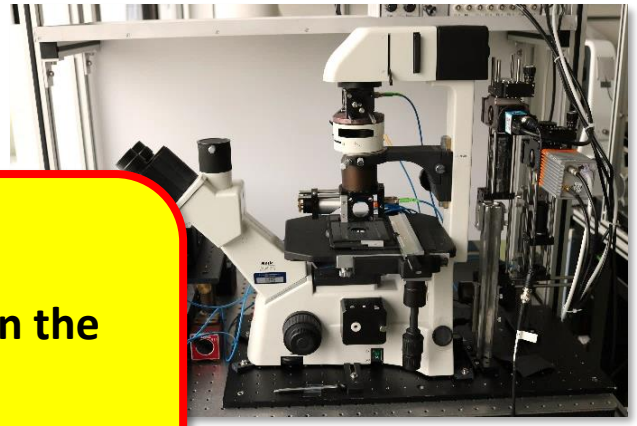

Laser-based DHM

Dust, particles and imperfections in the optical imaging system

➔ Cause parasitic interference patterns and coherence induced noise

suspended cells

phenotyping,
cell culture quality control

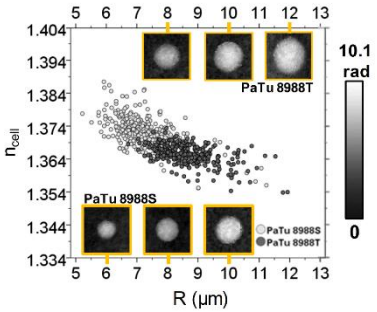

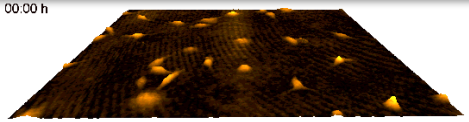

automated cell tracking

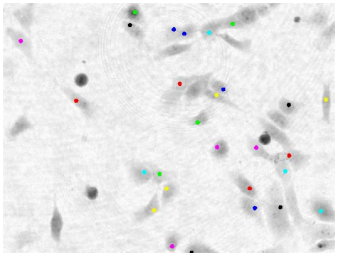

issue slices

tification of inflammation
mediated tissue sections

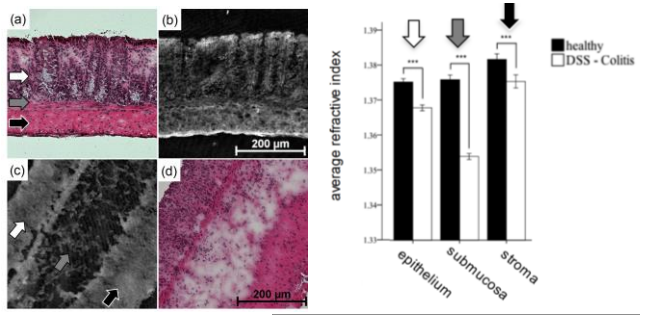

Concept for enhancement of QPI
(compatible with off-axis DHM and inverted research microscopes)

Object wave modulation with electrically focus tunable lens (EFTL)

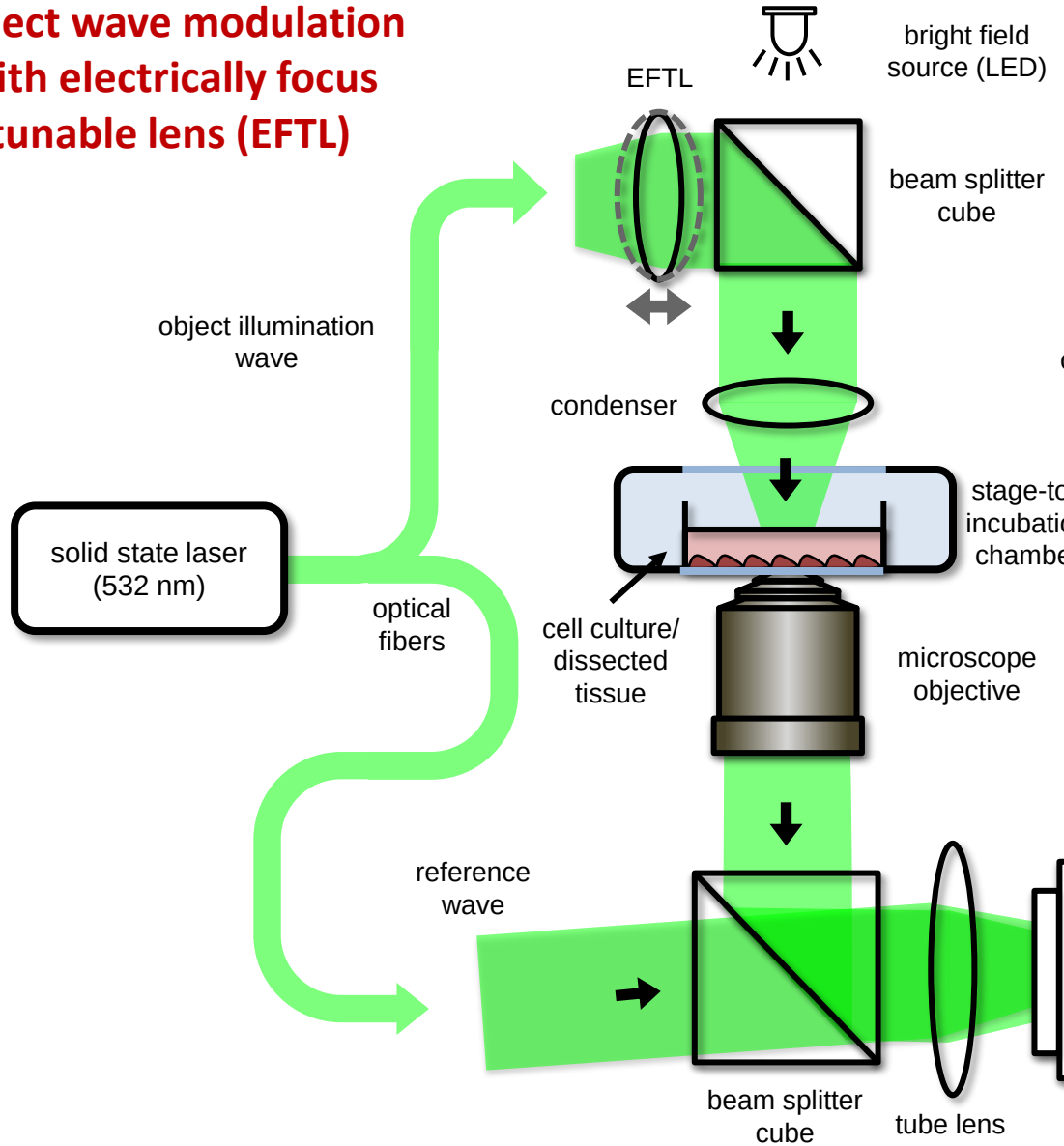

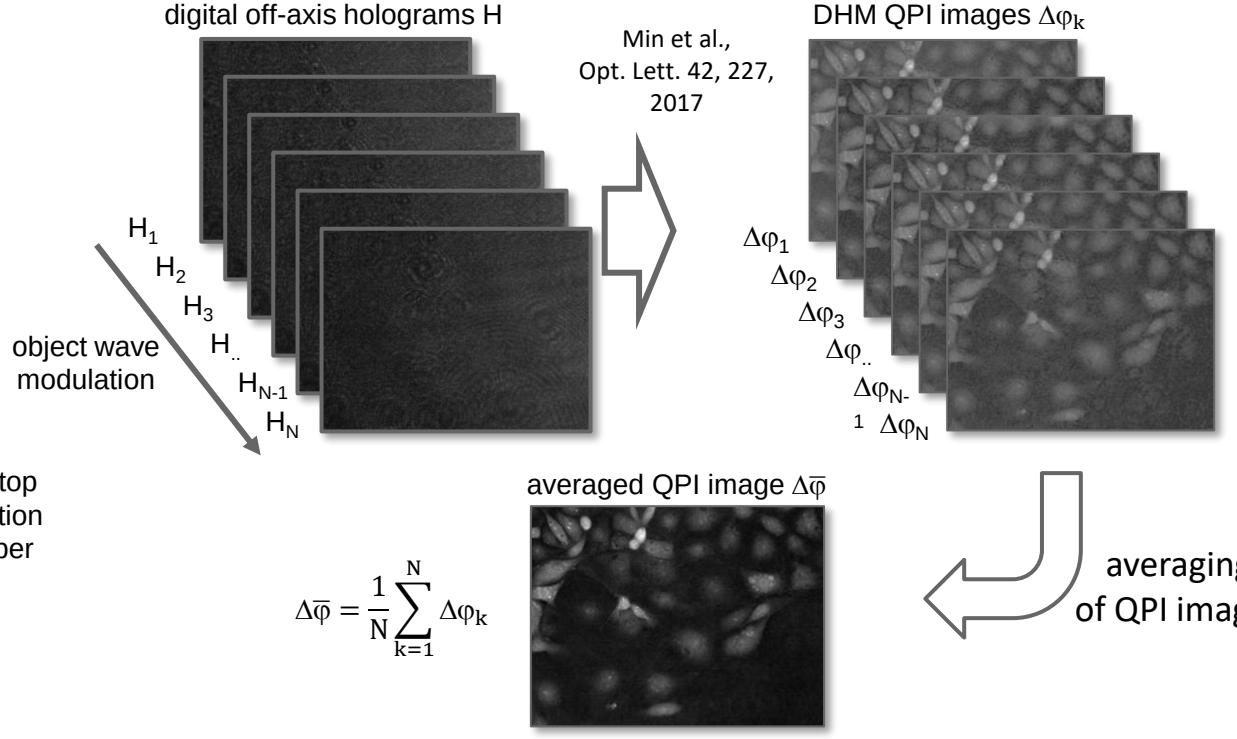

$$\Delta\bar{\varphi} = \frac{1}{N}\sum_{k=1}^{N}\Delta\varphi_k$$

Reduction of coherence induced image disturbance ≈ 47 %

B. Kemper, et al., Proc. SPIE 11653, 116530A (2021)

DHM QPI of living cells

Chinese hamster ovary (CHO) cells internalize silica SiO_2 particles by phagocytosis

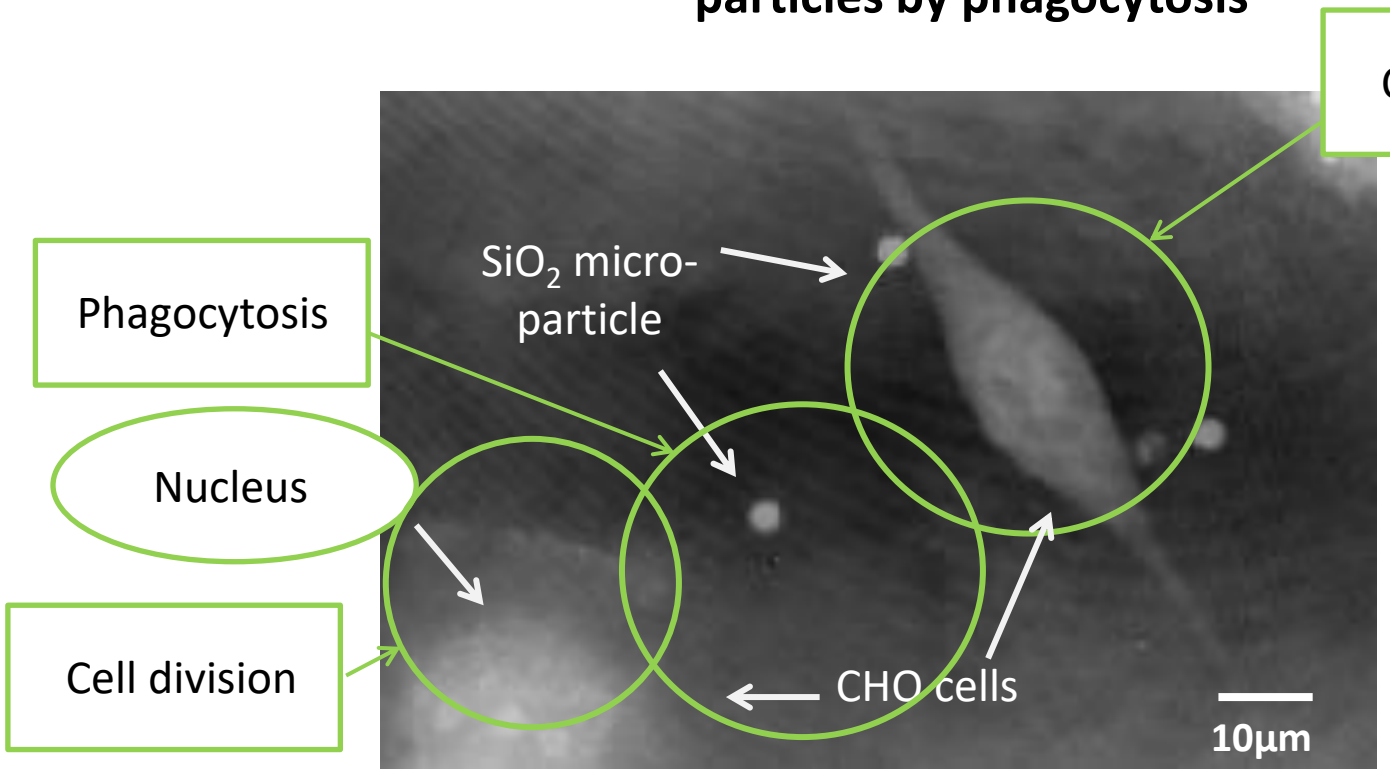

www.photonikforschung.de

B. Kemper, S. Przibilla, A. Vollmer, S. Ketelhut, G. von Bally, Imaging & Microscopy 1/2012, 19-21 (2012)
S. Przibilla, S. Dartmann, A. Vollmer, S. Ketelhut, G. von Bally, B. Kemper, J. Biomed. Opt. 17, 097001 (2012)

Example: Dynamic label-free DHM imaging of cardiomyocytes

Stimulation with isoprotenerol

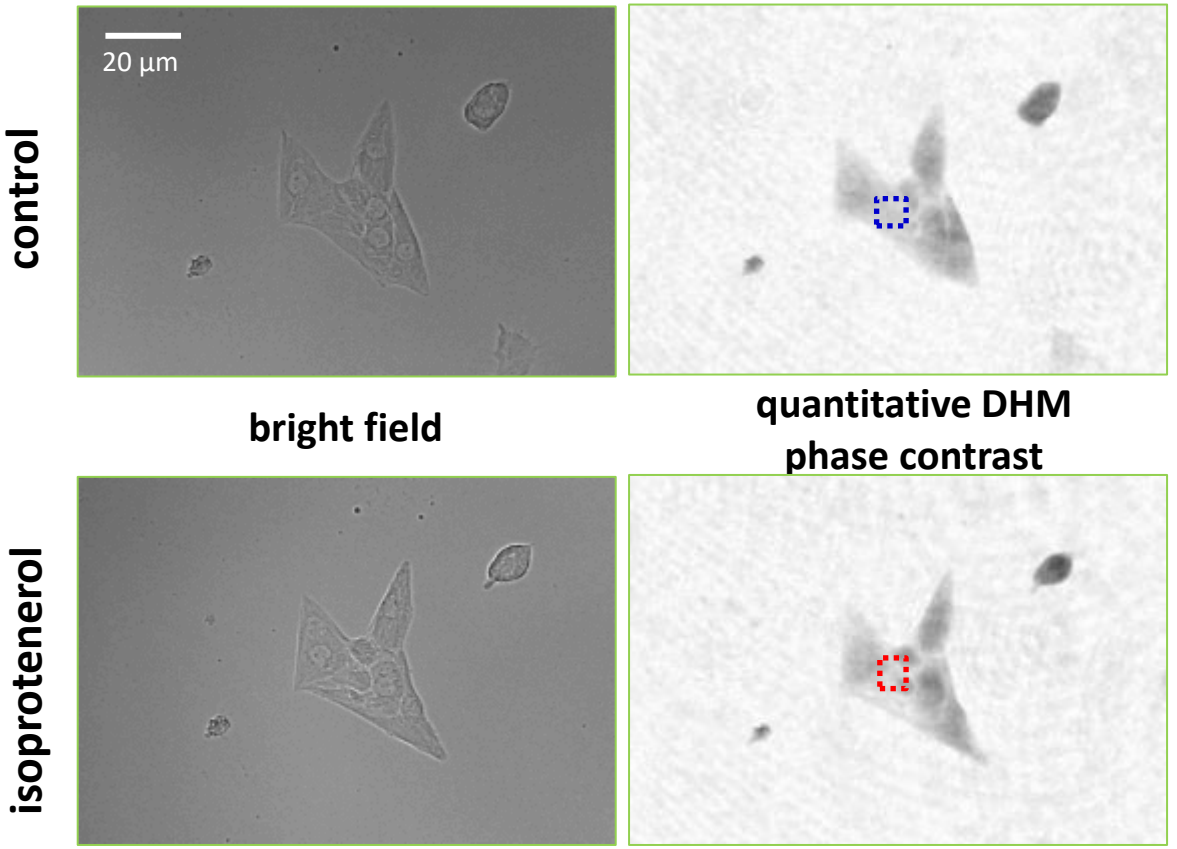

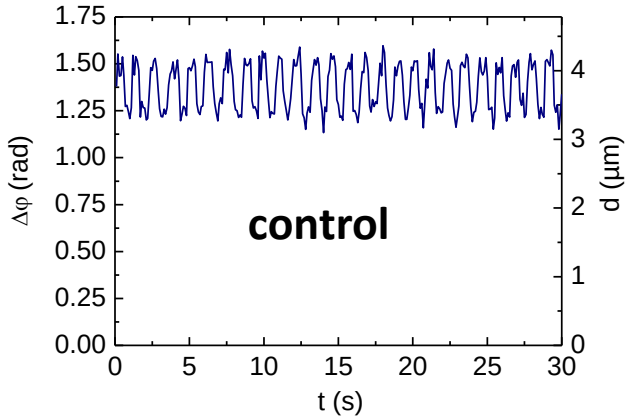

cell thickness

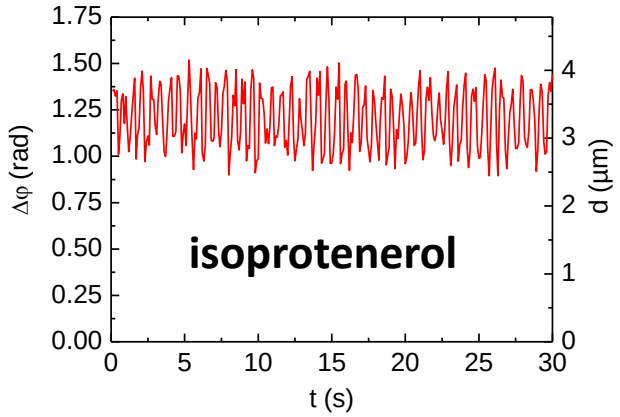

➔Increased contractility

20x

B. Kemper et al. Proc. SPIE 11249, 112491S (2020).

Multi-focus imaging and z-location of cells in suspension

amplitude stack
from a single hologram

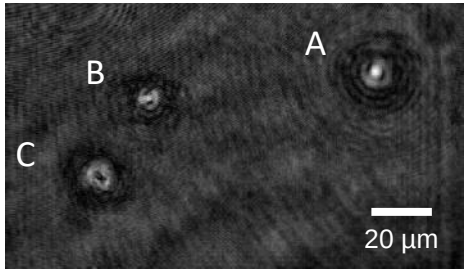

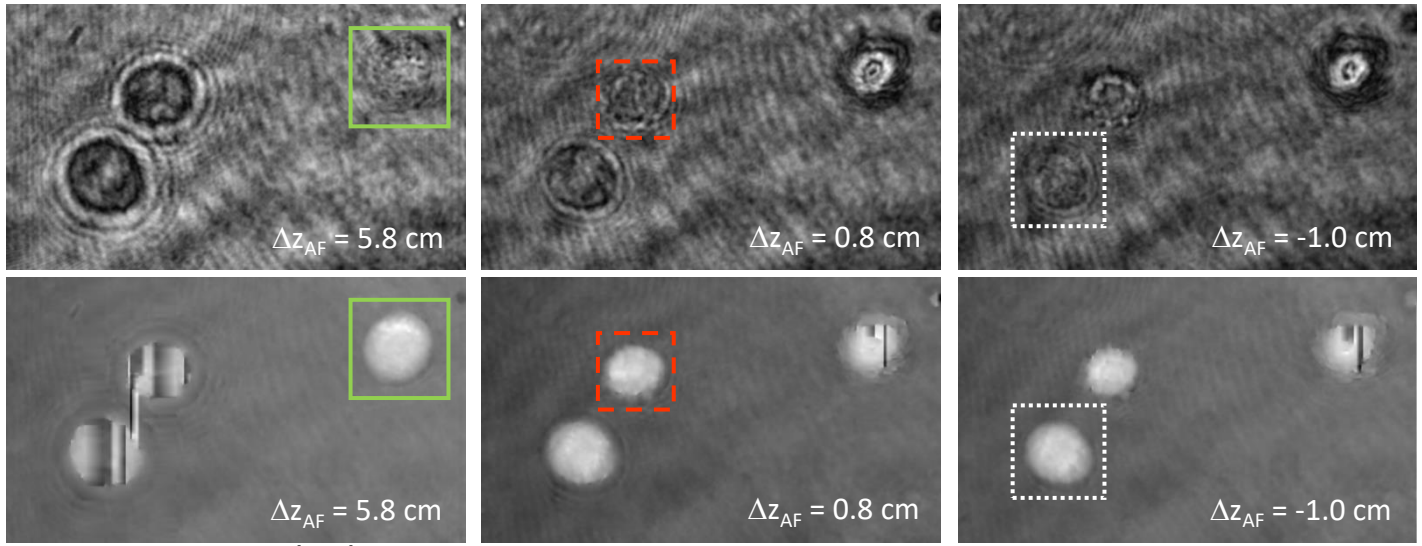

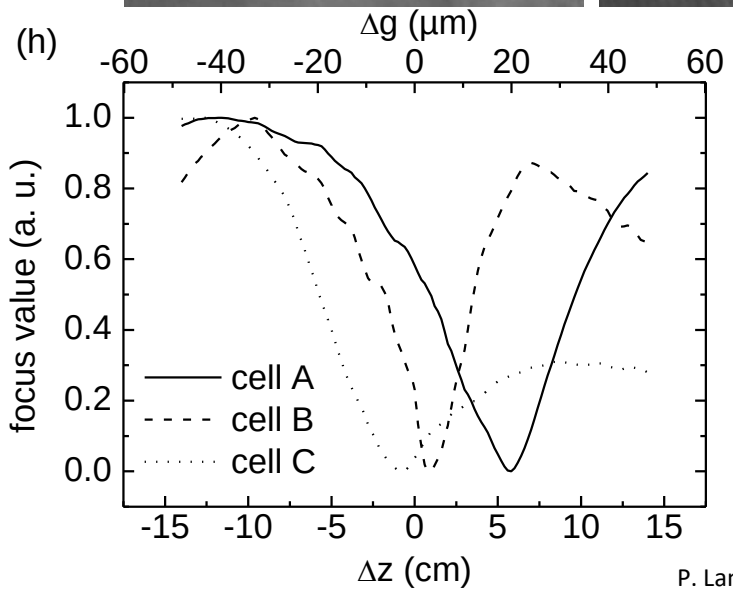

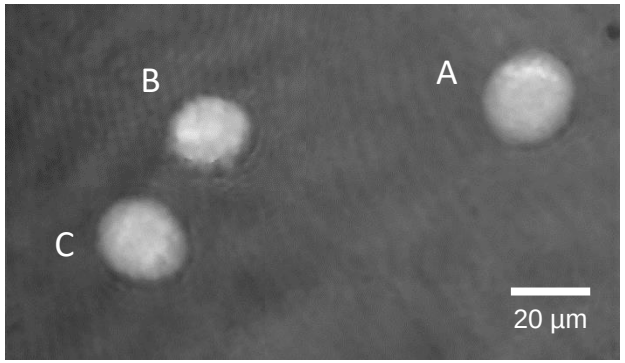

merged phase contrast image
➔ "enhanced depth of field"

P. Langehanenberg, G. von Bally, B. Kemper, 3D Res. 2, 01004 (2011)

BIOMED
BioMedizinisches
Technologiezentrum TECH

Extraction of biophysical parameters (illustrated by selected applications)

QPI-based label-free quantitative monitoring in-vitro migration / wound healing assays

Examples for preparation

1

Petri dish
with confluent
cell layer

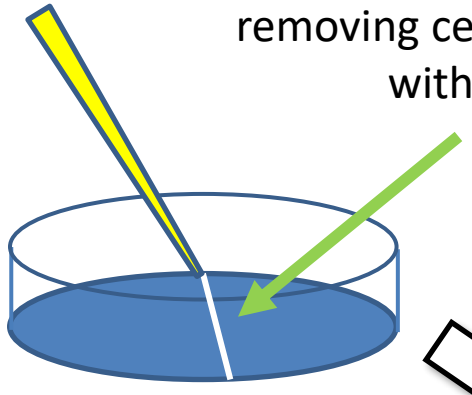

removing cell in specific area
with „scratch“

➔ monitoring of
cell migration into tissue gap

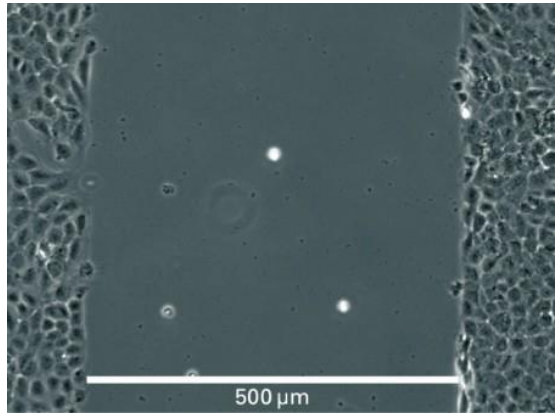

bright field Zernike phase contrast

2

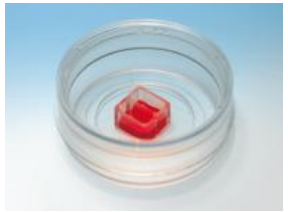

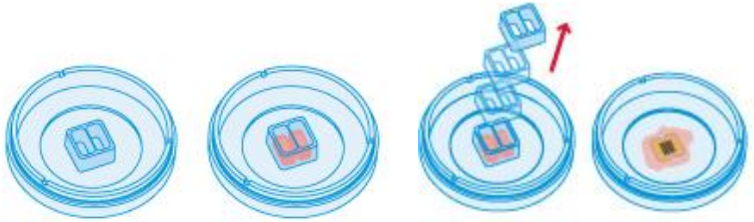

www.ibidi.com

www.ibidi.com

QPI-based label-free quantitative monitoring in-vitro migration / wound healing assays

BIOMED TECH
BioMedizinisches Technologiezentrum

Example: human fibro sarcoma cells, HT1080

phase contrast image: $\Delta\varphi_{\text{cell}}(x,y)$

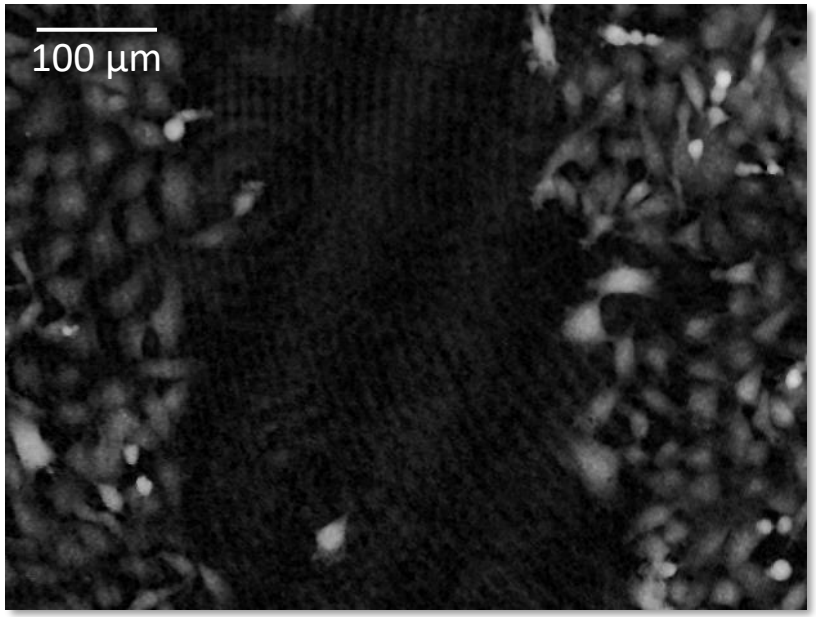

segmentation ➔ S_c, $\Delta\bar{\varphi}_{\text{cell}}$

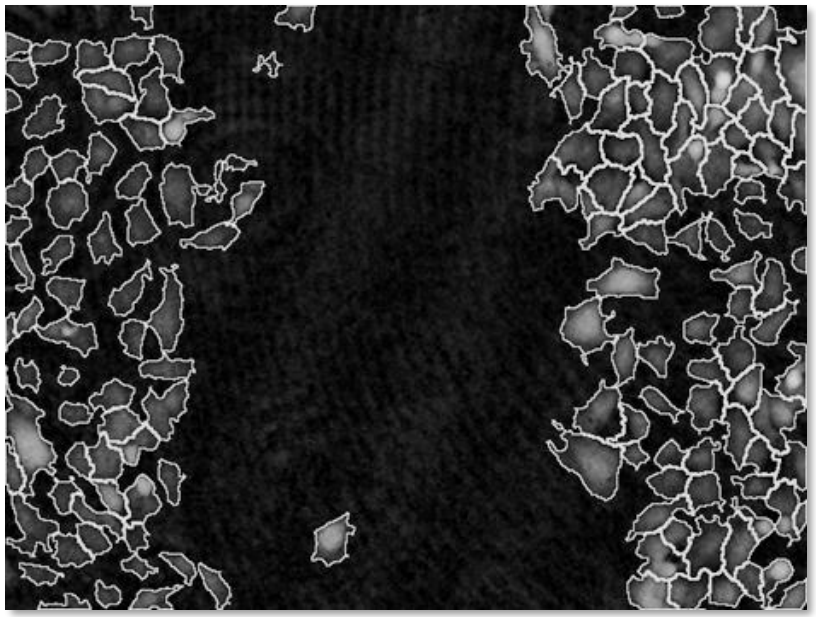

area covered by cells

S_c

dry mass

$$\mathrm{DM} = \frac{10\lambda}{2\pi\alpha}\int_{S_c}\Delta\varphi_{\text{cell}}\,ds = \frac{10\lambda}{2\pi\alpha}\Delta\bar{\varphi}_{\text{cell}}\,S_c$$

$\alpha \approx 0{,}0002$ m³/kg

average cell thickness

$$\bar{d}_{\text{cell}} = \frac{\lambda\Delta\bar{\varphi}_{\text{cell}}}{2\pi}\cdot\frac{1}{\left|n_{\text{cell}} - n_{\text{medium}}\right|}$$

10x, λ = 532 nm

Barer, Nature (1952), Rappaz et al., JBO (2009), Mir et al. PNAS (2011)

QPI-based label-free quantitative monitoring of in-vitro migration / wound healing assays

BIOMED TECH
BioMedizinisches Technologiezentrum

quantitative DHM phase images

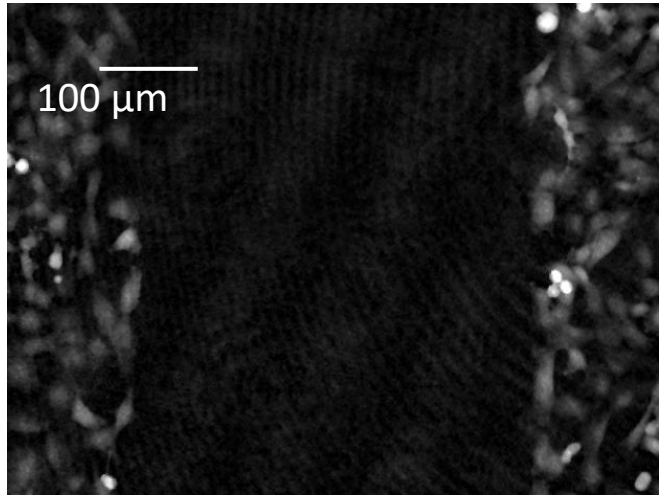

image segmentation

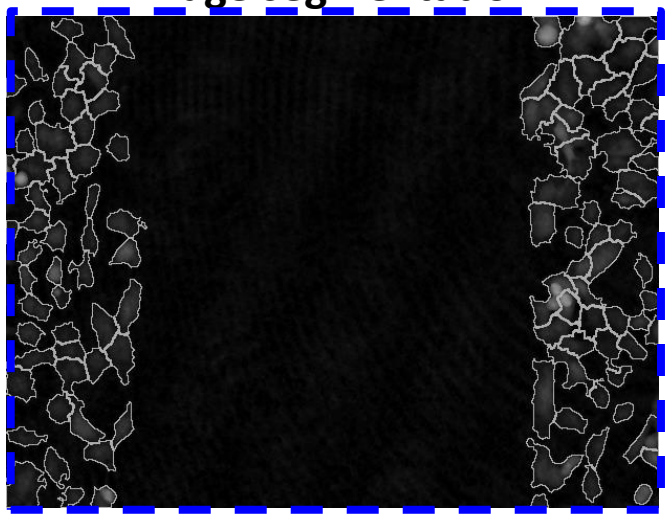

t = 0 – 24 h
Δt = 3 min

averaging

area covered by cells

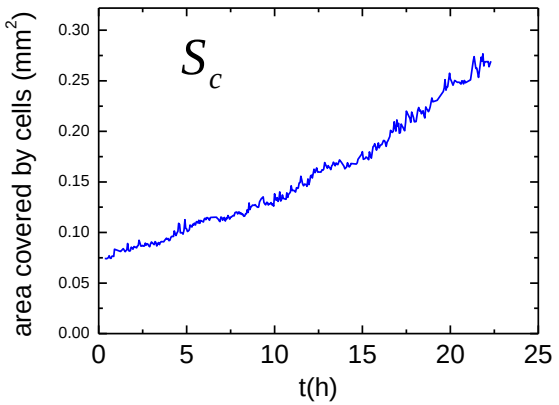

dry mass

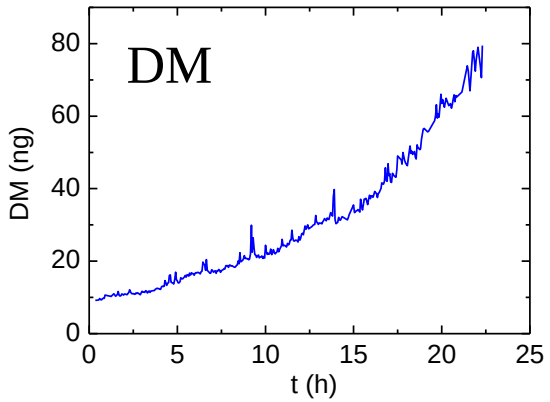

mean cell culture thickness

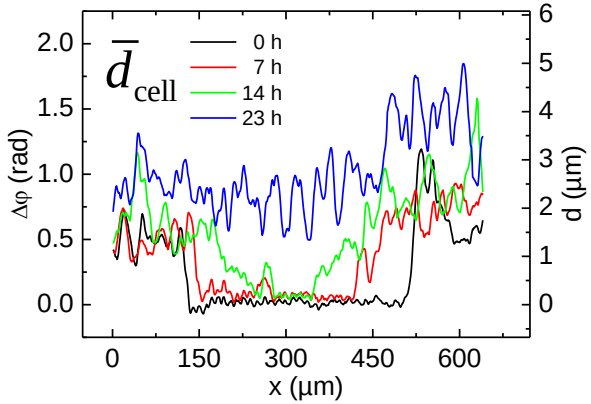

10x,NA=0.25, 532 nm

D. Bettenworth, P. Lenz, P. Krausewitz, M. Brückner, S. Ketelhut, G. von Bally, D. Domagk, B. Kemper, Proc. SPIE 8797, 879702 (2013)
D. Bettenworth, D. Bettenworth, P. Lenz, P. Krausewitz, M. Brückner, S. Ketelhut, D. Domagk, B. Kemper, PLOS ONE 9, 07317 (2014).
D. Bettenworth, A. Bokemeier, C. Poremba, N. S. Ding, S. Ketelhut, P. Lenz, B. Kemper, Histol. Histopathol. 33, 417-432 (2018)

BIOMED TECH
BioMedizinisches Technologiezentrum

Automated cell tracking

QPI-based automated 2D cell tracking

BioMed BioMedizinisches Technologiezentrum TECH

Software

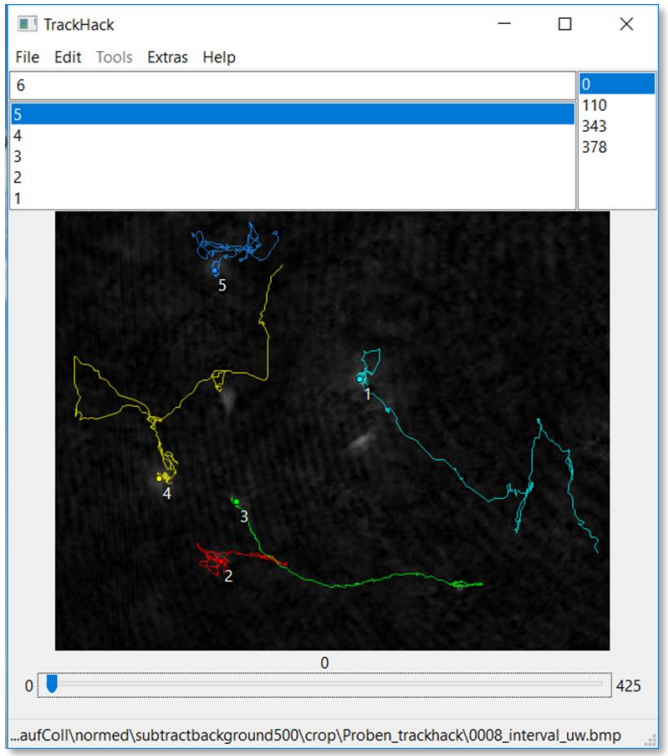

Cell tracking by detection of the maximum cell induced phase contrast

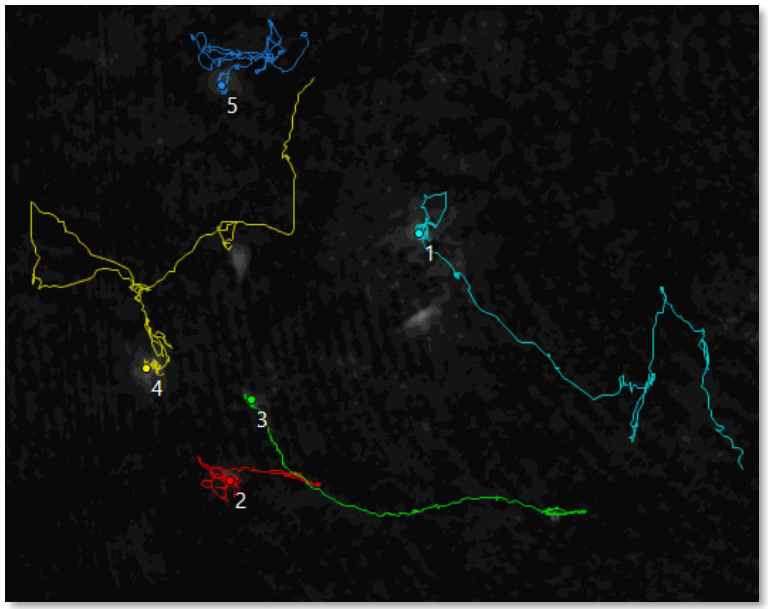

10x, NA=0.3, 532 nm

➔ Fast automated cell tracking (e.g., 800 images in ≈ 1-2 sec)

➔ extraction of various migration related parameters (Mean squared displacement, max. migration distance, FMi, directness, velocity, …)

Cell tracking procedure: B. Kemper, et al., J. Biomed. Opt. 15, 036009 (2010)

Quantification of cell motility

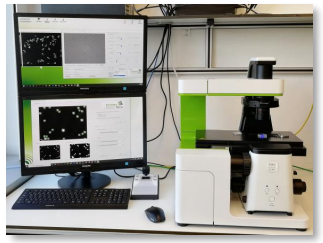

Bright field bright field time-lapse observation of pancreatic tumor cells

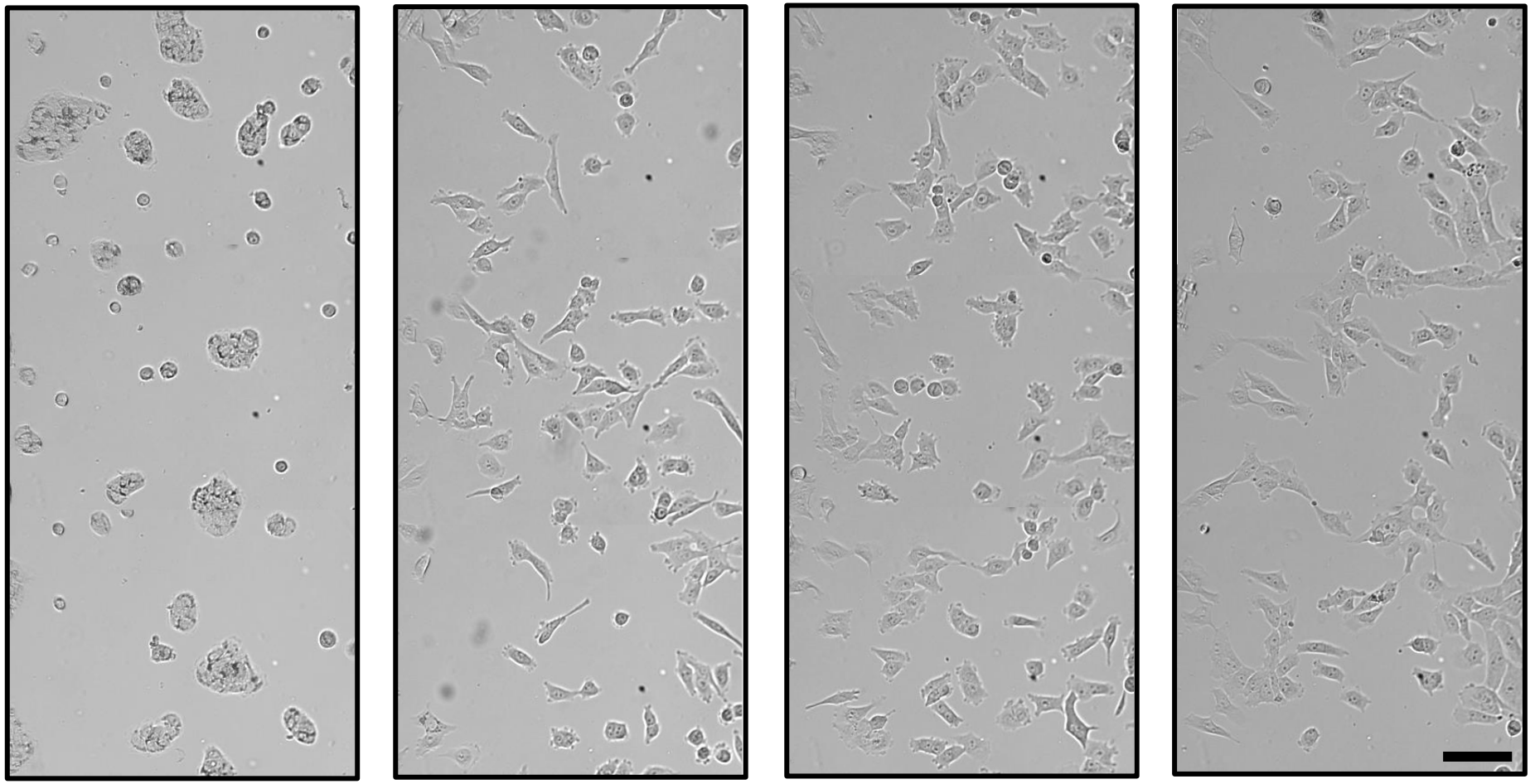

Stitched images recorded a different fields of view (20x), t = 12 h

Determination of cell motility

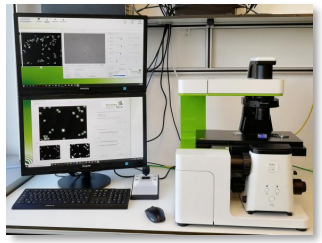

Quantitative DHM Phase images of pancreatic tumor cells

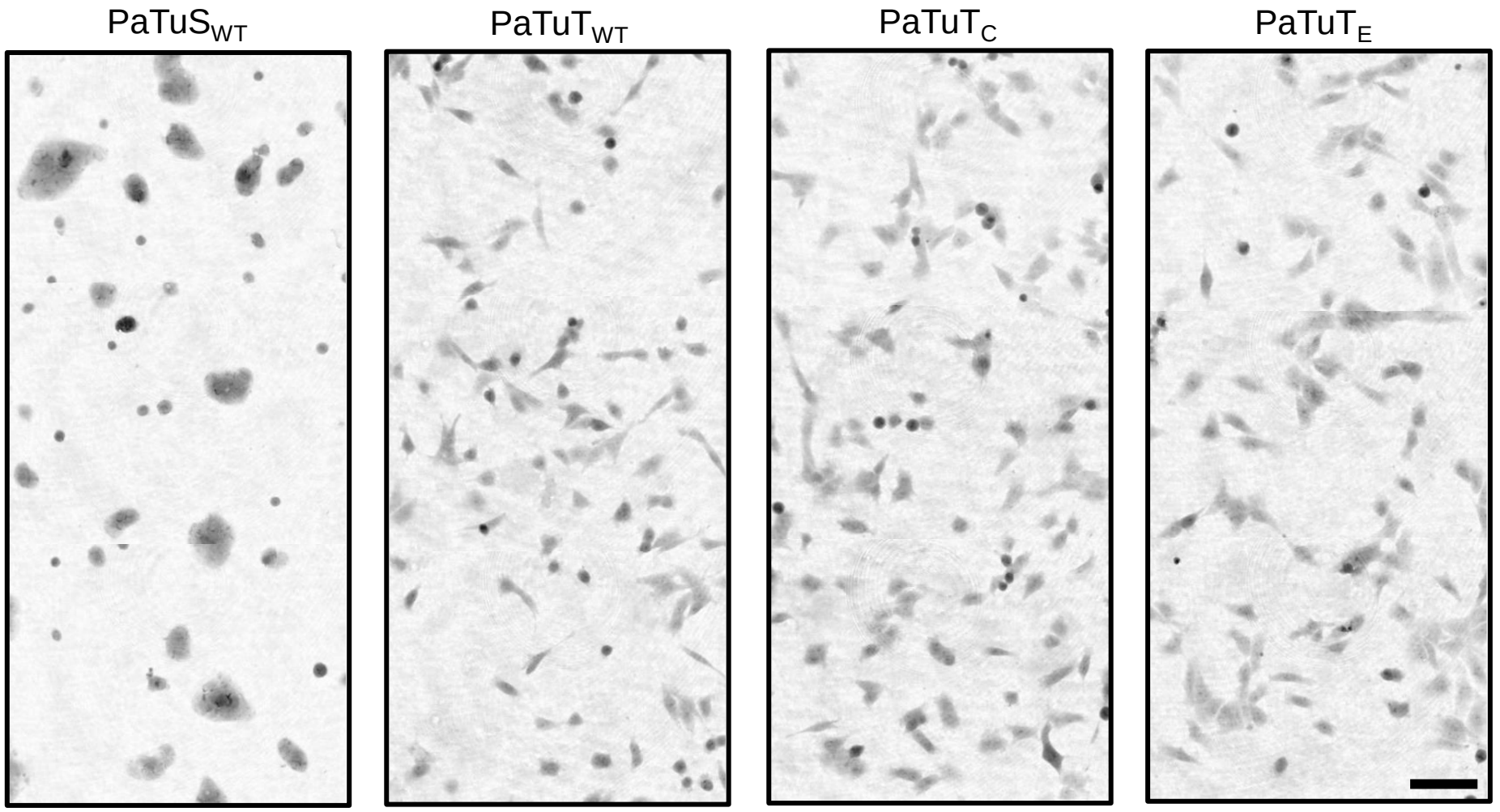

Stitched images recorded a different fields of view (20x), t = 12 h

Determination of cell motility

BIOMED TECH
BioMedizinisches Technologiezentrum

DHM-based retrieval of migration trajectories of pancreatic tumor cells

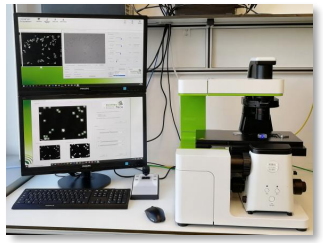

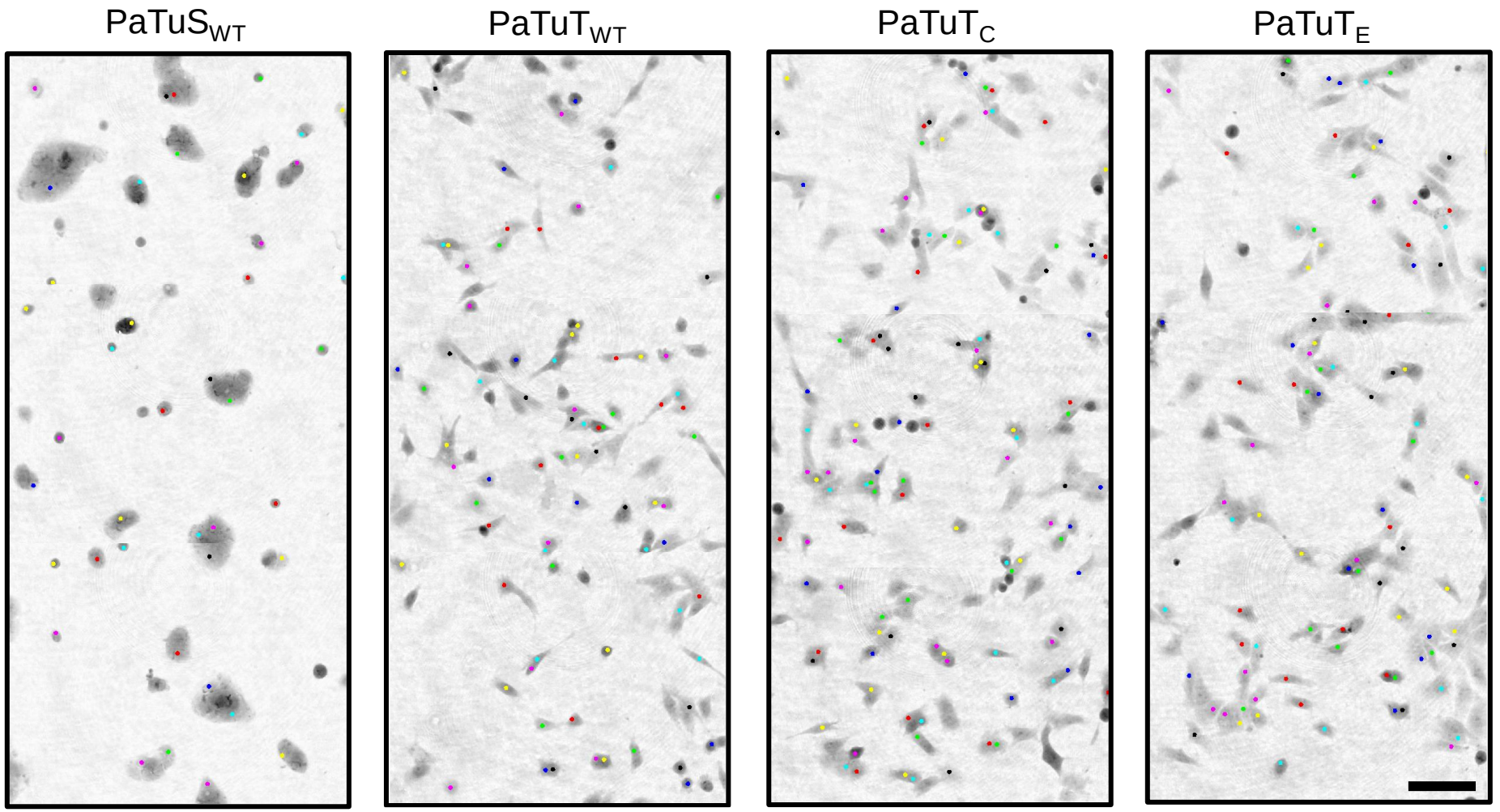

Stitched images recorded a different fields of view (20x), t = 12 h

Determination of cell motility

Migration trajectories of pancreatic tumor cells

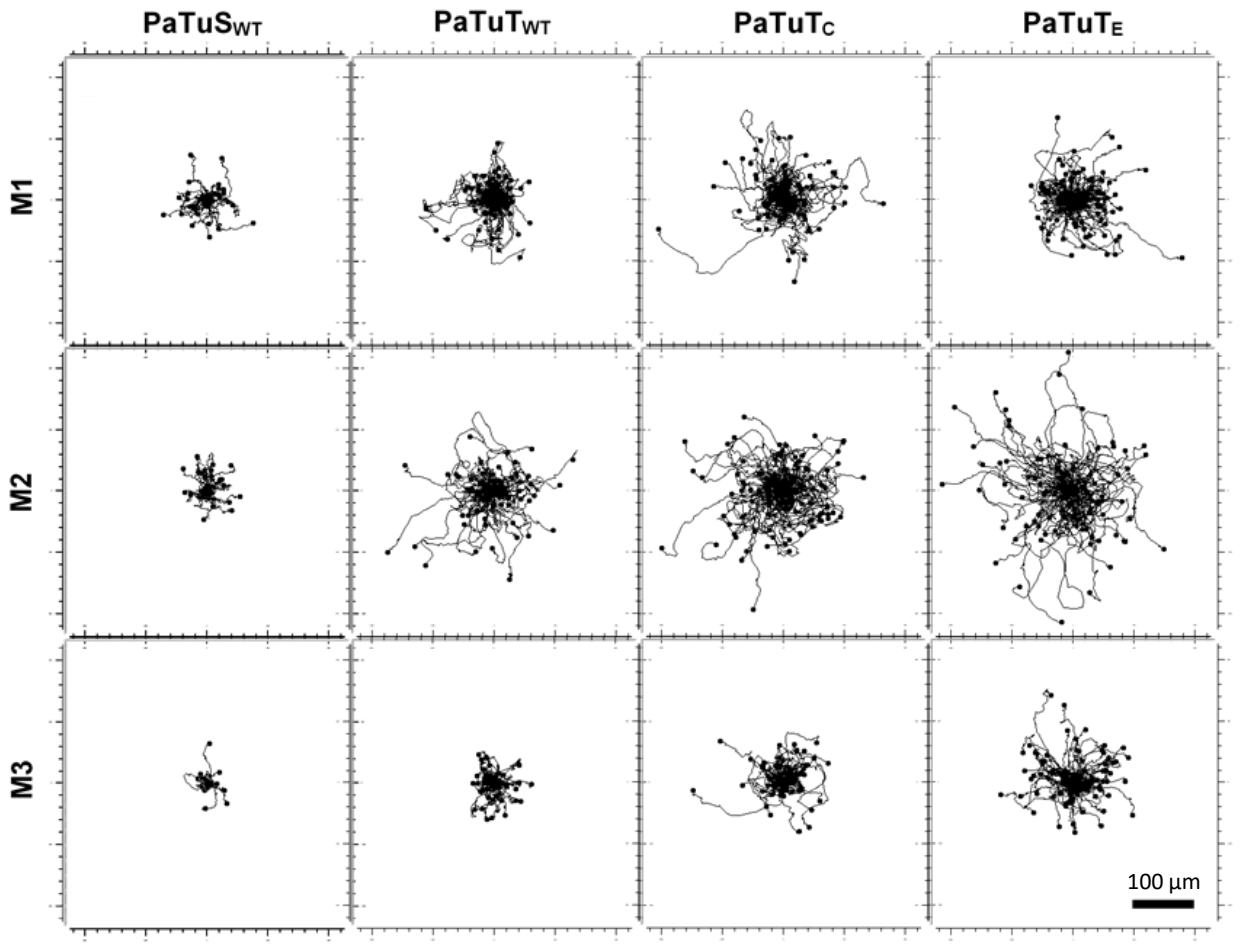

t = 12 h, N=3 independent experiments (M1-M3)

Plots created with ibidi chemotaxis and migration Tool (www.ibidi.com)

Accumulated distance

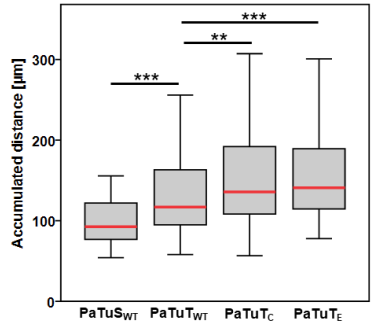

Euclidian distance

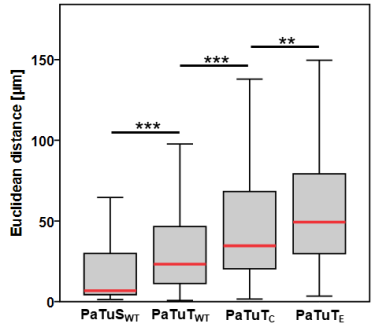

Directness

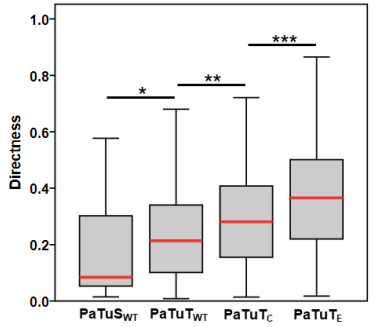

BIOMED
BioMedizinisches
Technologiezentrum
TECH

Multimodal / multiparameter imaging

Multi-parameter analysis of breast cancer cells

Influence of VE-cadherin on cell migration and morphology

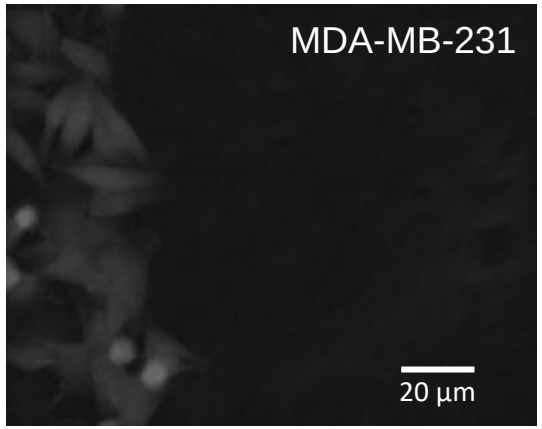

quantitative DHM phase contrast

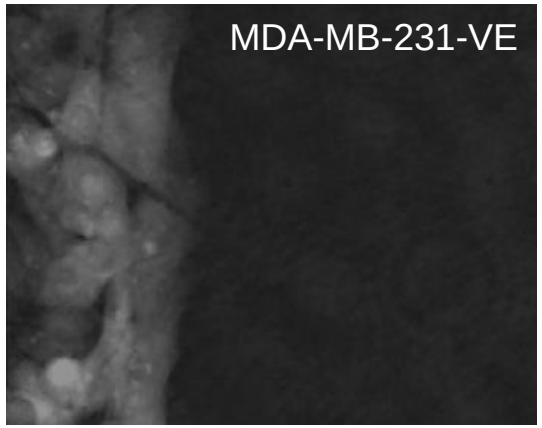

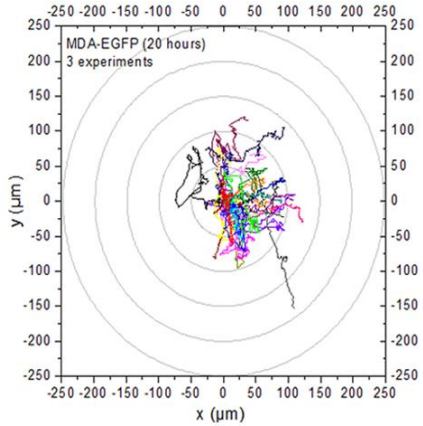

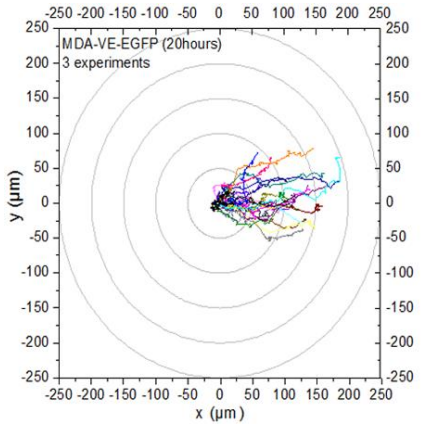

migration trajectories

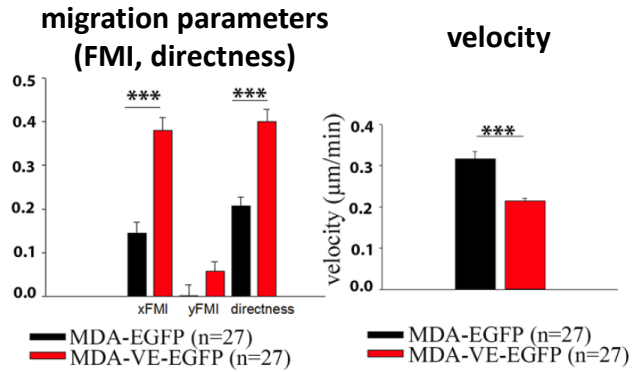

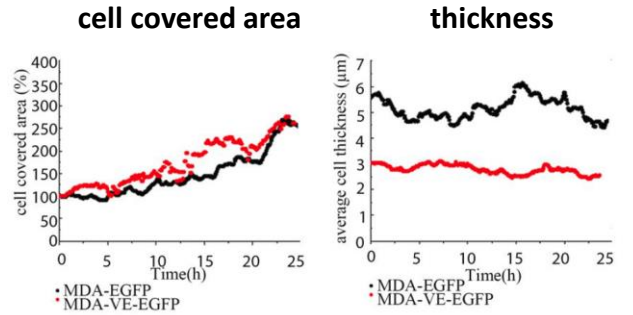

M. Rezaei et al.
Histochemistry and Cell Biology Histochem. Cell Biol. 149, 15-30 (2018)

➔ **Significant change of migration direction, velocity and cell thickness**

DHM Principle: Schubert et al., Biomed. Opt. Express 5, 4213-4222 (2014); Cell Tracking Procedure: Kemper et al., J. Biomed. Opt. **15**, 036009 (2010)

BIOMED
BioMedizinisches
Technologiezentrum TECH

Suspended cells:

Determination of integral cellular refractive index, volume, and dry mass

Refractive index, volume and dry mass characterization suspended single cells

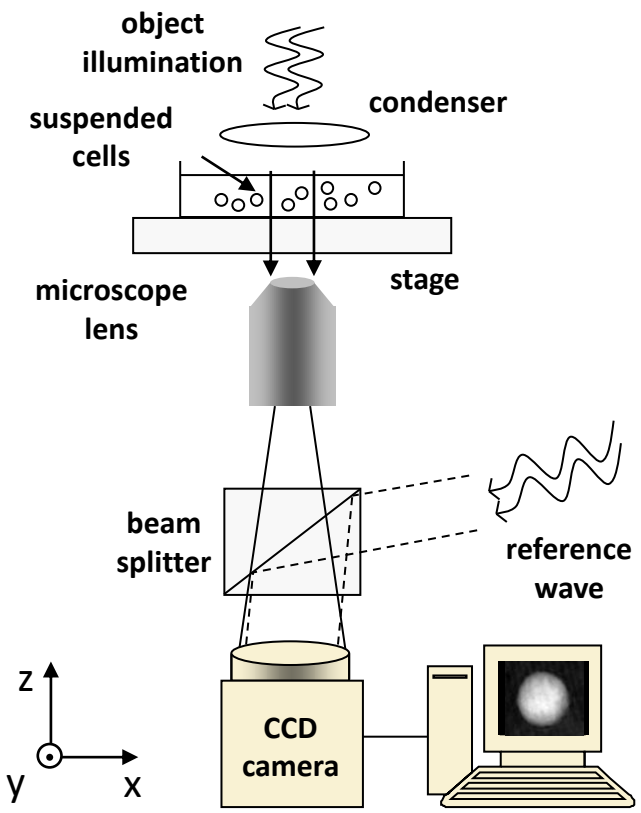

required: n_{medium} and imaging scale

n_{cell} ~ intracellular solute concentration

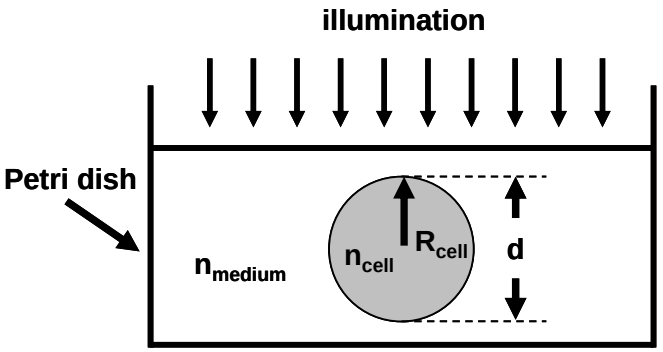

phase change: spherical cell

$$\Delta\varphi_{cell}(x,y) = \frac{4\pi}{\lambda}(n_{cell} - n_{medium}) \cdot \sqrt{R^2 - (x-x_0)^2 - (y-y_0)^2}$$

volume

$$V = \frac{4}{3}\pi R^3$$

$\alpha \approx 0.002\ \mathrm{m^3/Kg}$

dry mass

$$DM = \frac{V}{\alpha} \cdot (n_{cell} - n_{medium})$$

L. Kastl, et al., Cytometry Part A, DOI: 10.1002/cyto.a.23082 (2017)

DHM phase contrast image

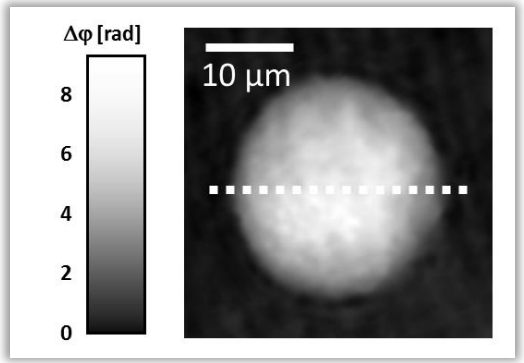

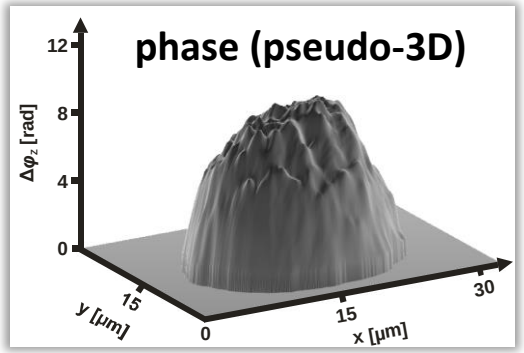

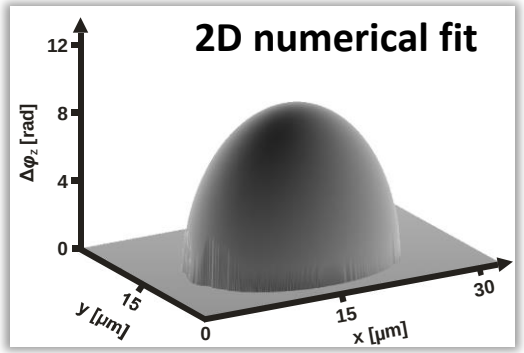

(Gauß-Newton/Levenberg Marquart)

Label-free analysis of suspended cells for phenotyping and cell culture quality control

BIOMED TECH
BioMedizinisches Technologiezentrum

Individual biophysical signatures of different cell types

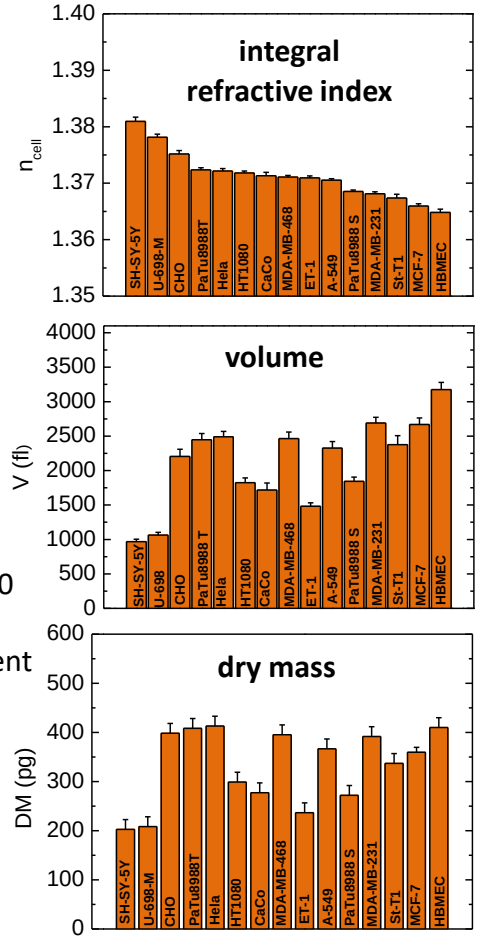

N=100-200 cells per measurement

B. Kemper, et al., Bioanalytical Reviews (2019), BIOREV (2019) 2: 219–272 (Springer).

Volume, refractive index and dry mass determination

Example: pancreatic tumor cells

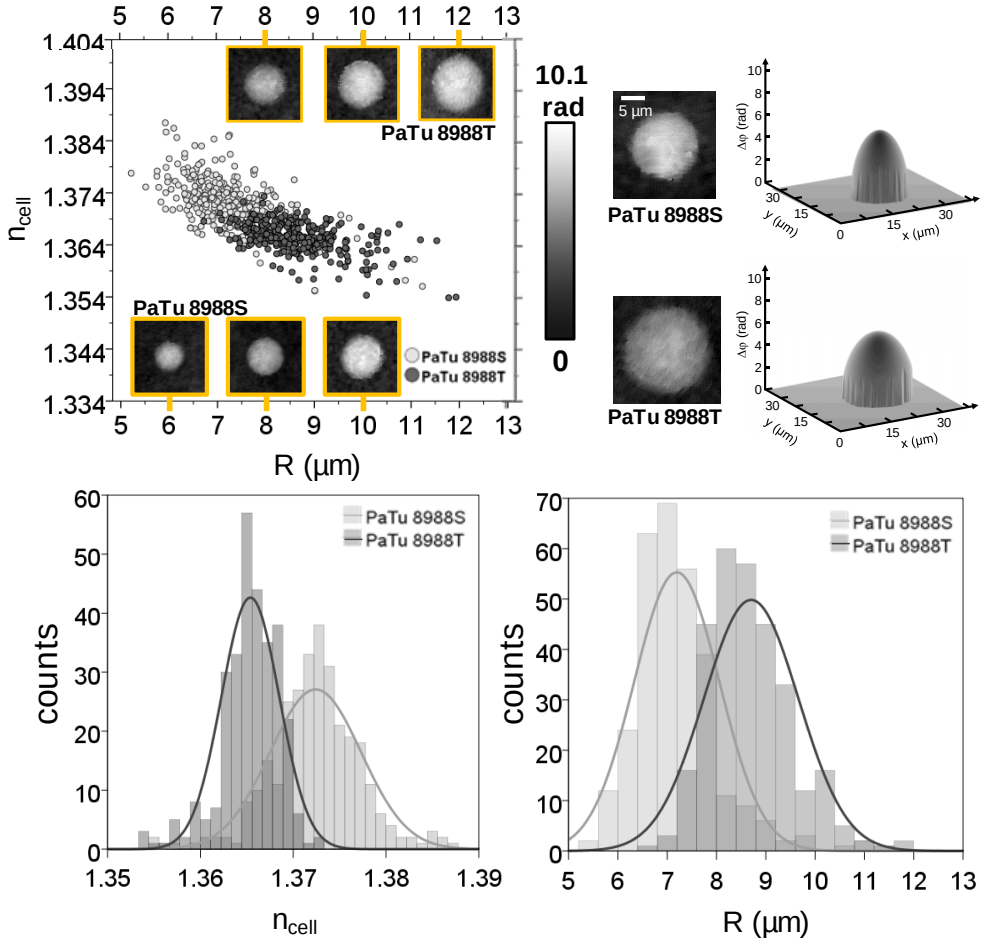

➔ **Significant cell radius and refractive index differences**

L. Kastl, et al., Cytometry Part A, DOI: 10.1002/cyto.a.23082 (2017)

High reliability / repeatability (N=3, independent measurement)

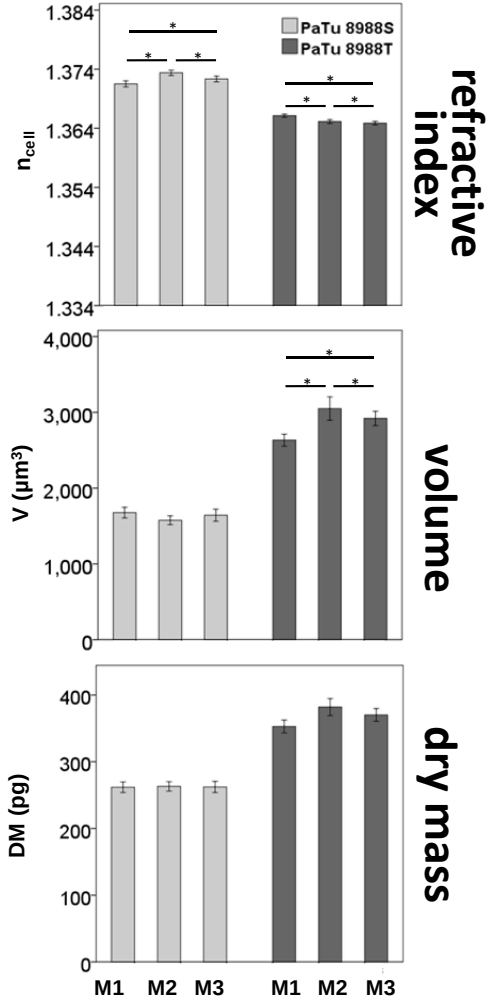

N = 100 cells per measurement

Towards automated cell analysis and image flow cytometry

BIOMED TECH
BioMedizinisches Technologiezentrum

Automated analysis of suspended cells in Petri dishes

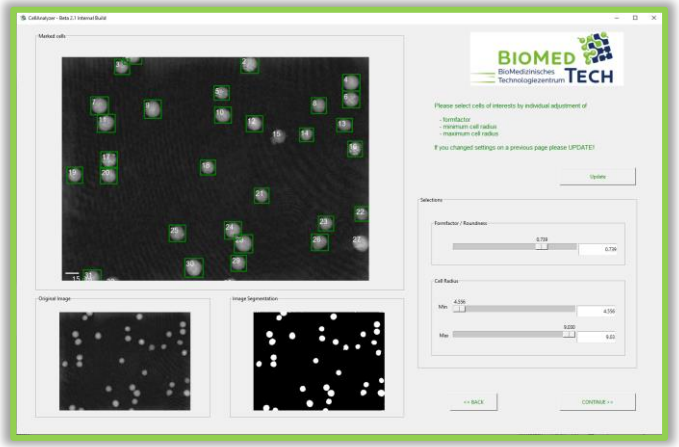

automated object recognition

segmentation

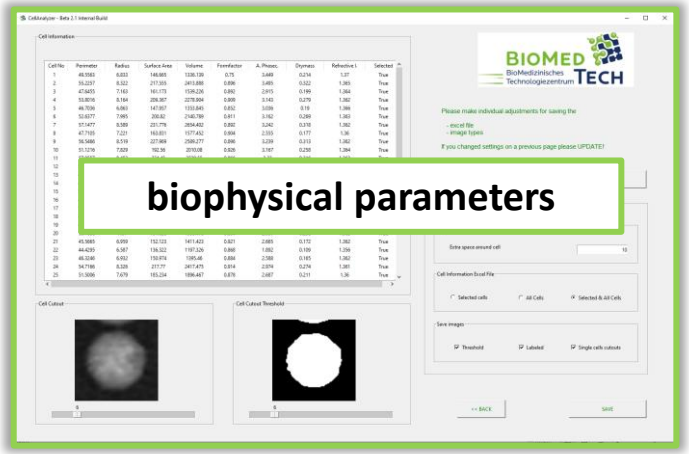

L. Brandt et al. Proc. BIOSTEC 2018 5, 431-437 (2018).

Holographic image flow cytometry of pancreatic tumor cells

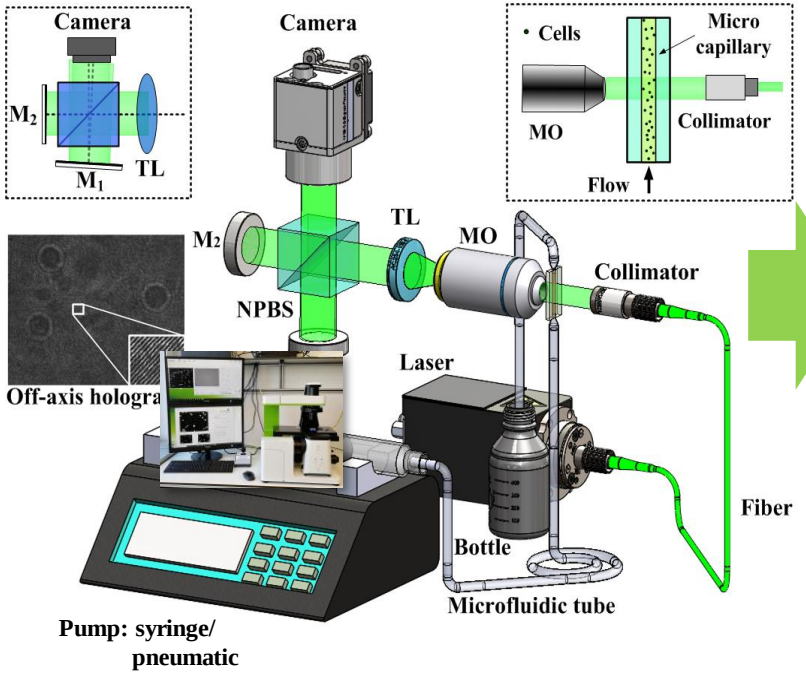

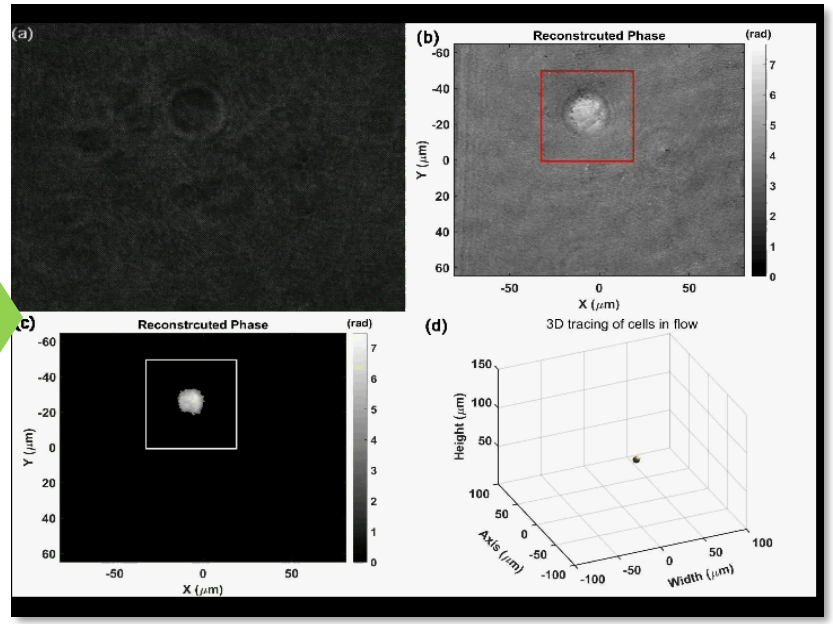

Refractive index (static, flow)

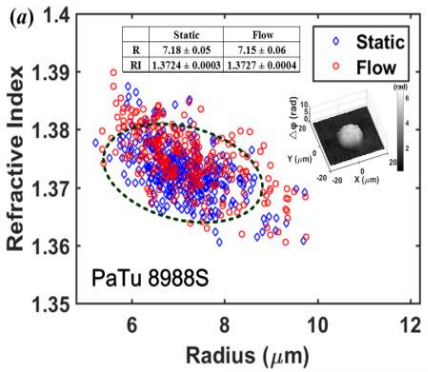

Cell mixture (flow)

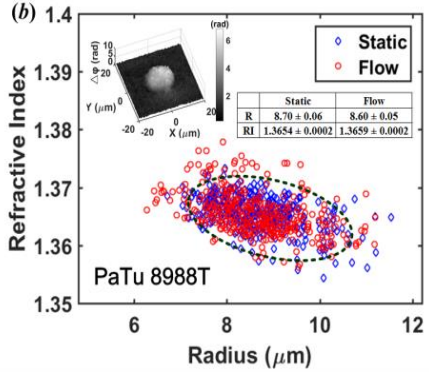

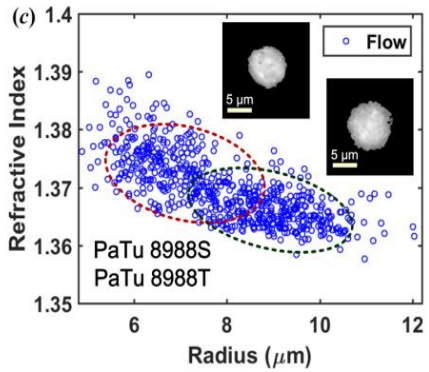

J. Min et al., J. Biophoton. 12, e201900085 (2019).

BIOMED
BioMedizinisches
Technologiezentrum
TECH

Toxicity testing

Time-lapse observation of the impact of toxic vesicles on human gastrointestinal cells (HCT-8)

t = 0-48 h

white light images

segmented quantitative DHM phase contrast images

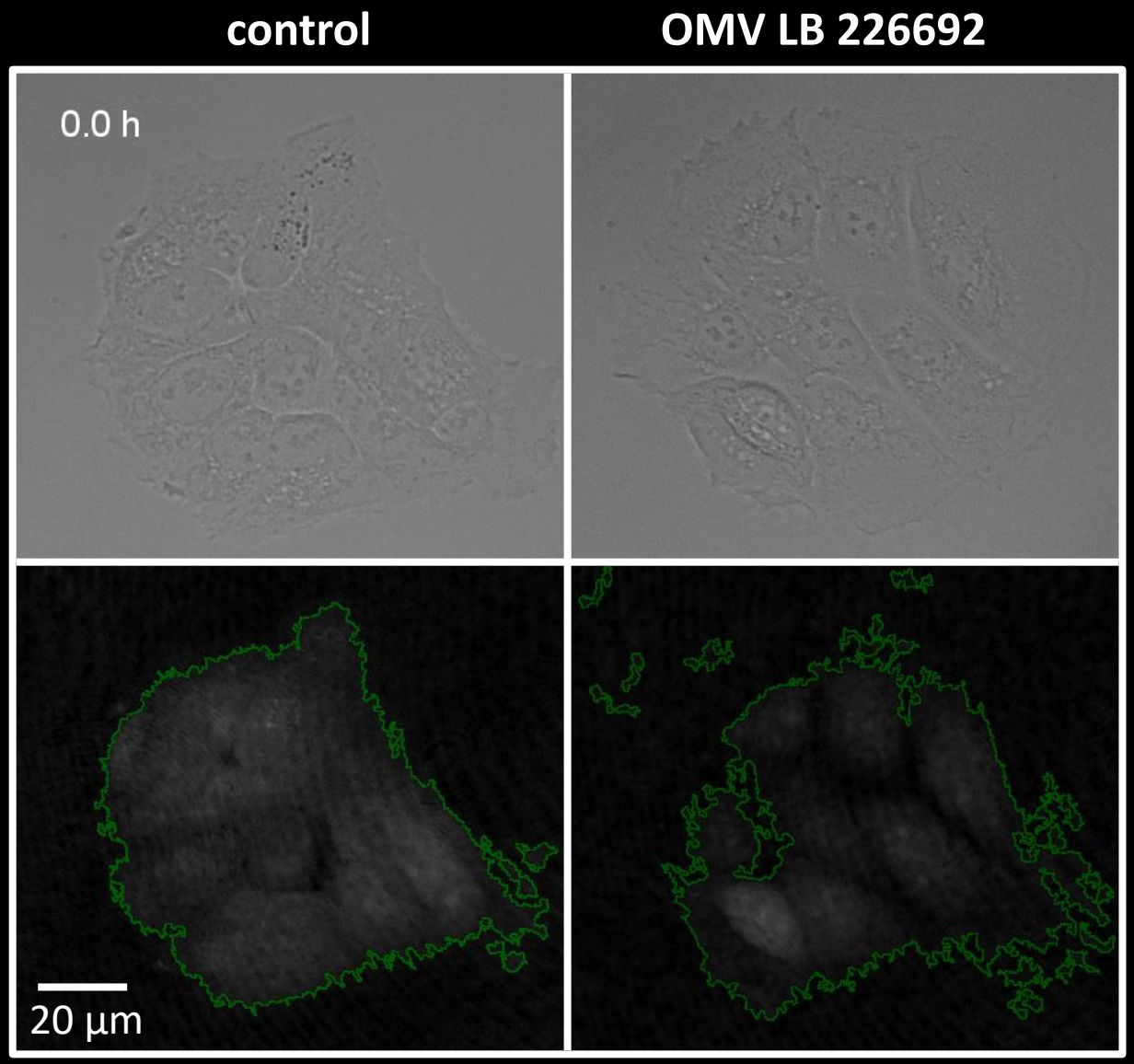

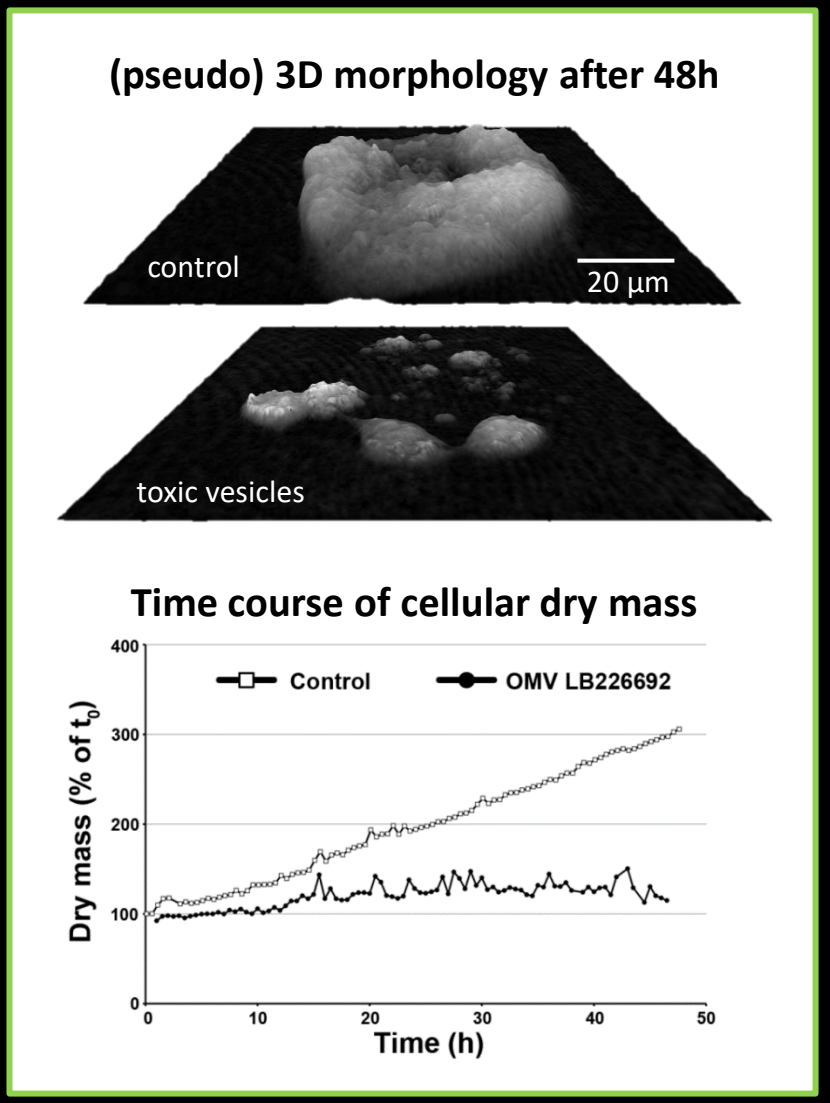

L. Kunsmann, et al., Sci. Rep. 5, 13252 (2015)

DHM QPI observation of macrophages (RAW264.7) after incubation with a cytotoxic silver nano material (NM 300)

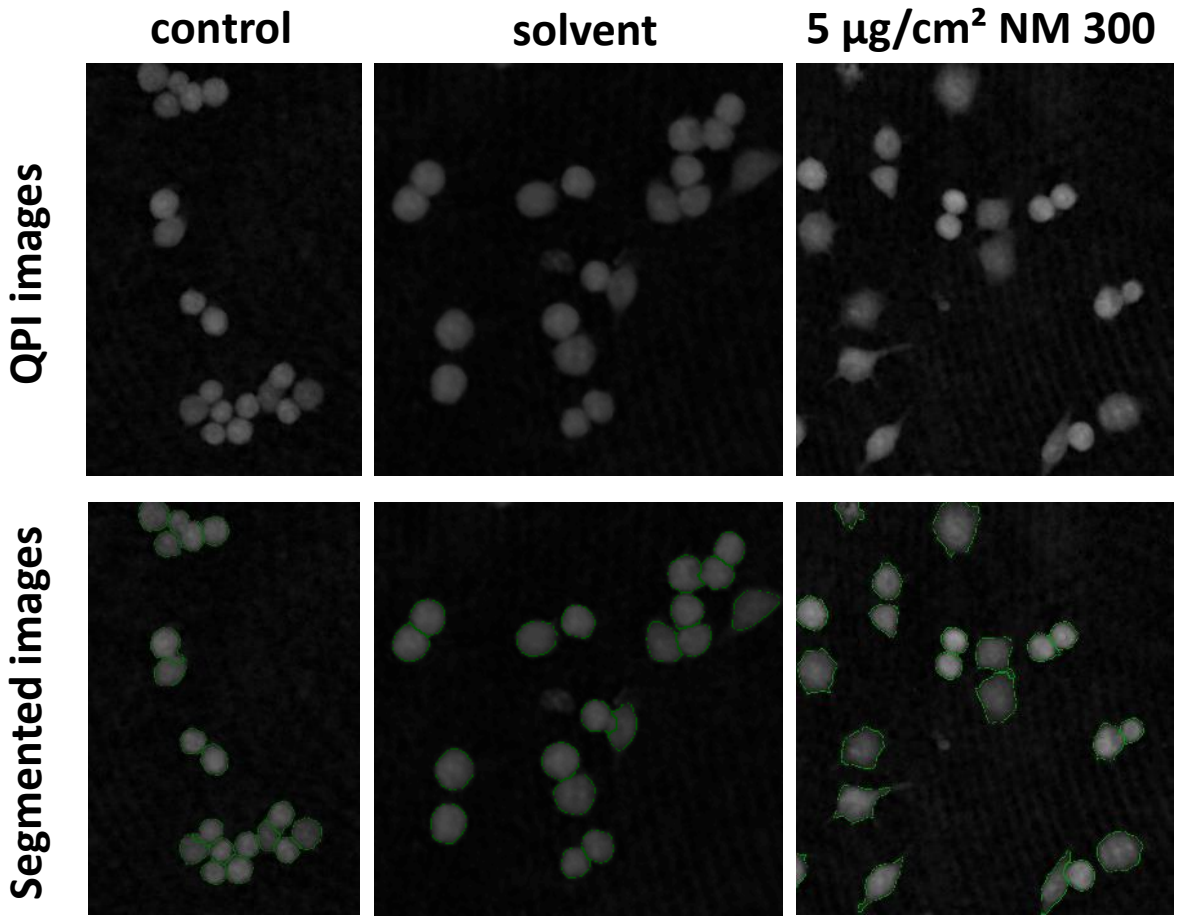

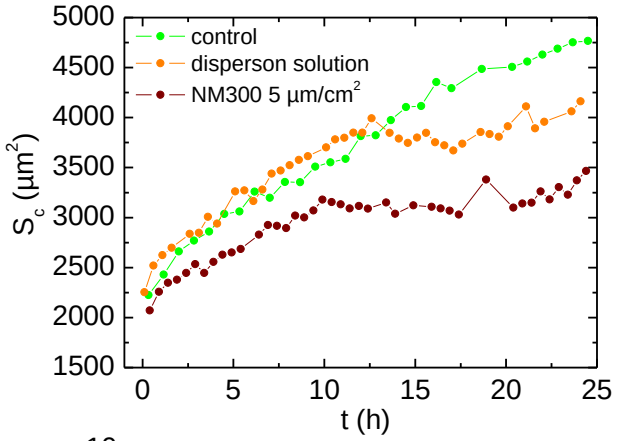

projected cell surface

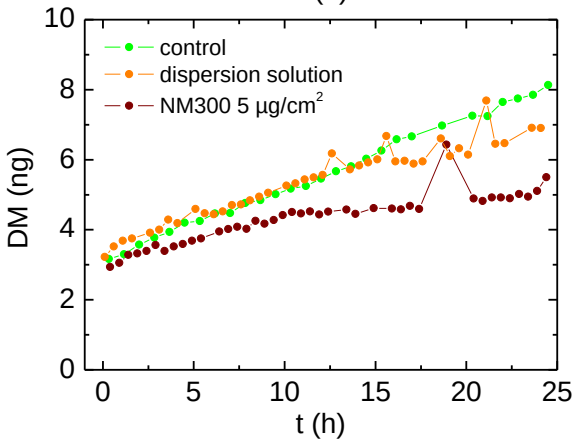

dry mass

➔ **Cytotoxic effects of silver nano spheres cause significant proliferation decrease**

B. Kemper, et al., BIOREV (2019) 2: 219–272 (Springer Nature Switzerland AG).

BIOMED
BioMedizinisches
Technologiezentrum
TECH

Quantitative imaging of tissue sections

Example: Experimental colitis in mice
Refractive index corelates with degree of inflammation

BIOMED TECH
BioMedizinisches Technologiezentrum

DHM analysis of cryostat tissue sections (mouse colon, d = 7 µm)

epithelium

submucosa

stroma

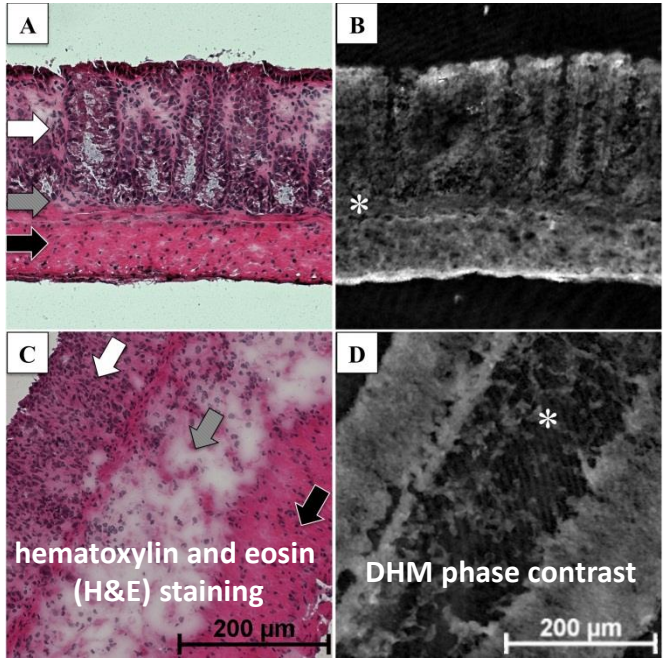

$$n_s(x,y) = \left(\frac{\Delta\varphi_s(x,y)}{d}\frac{\lambda}{2\pi}\right) + n_{\text{medium}}$$

➔Towards absolute parameters in “digital pathology”

refractive index / density map

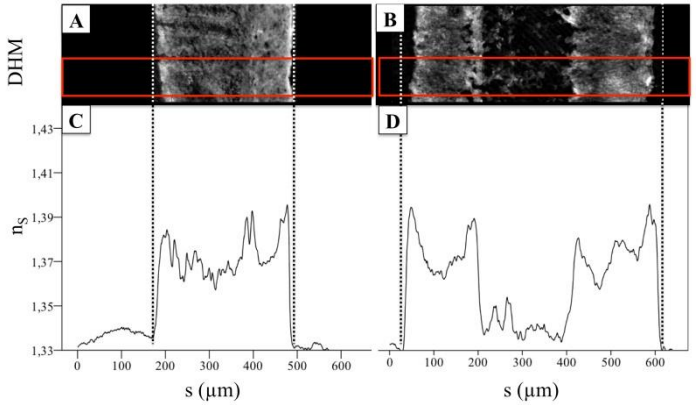

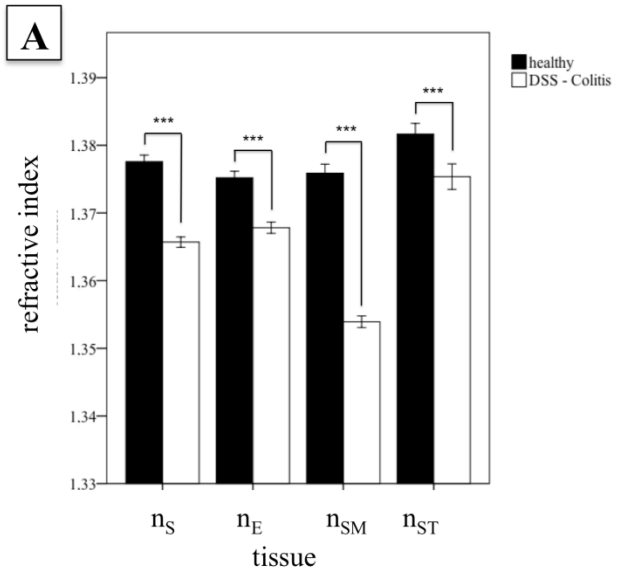

10 healthy animals
10 colitis animals

75 measurements per animal

➔ significant density loss due to inflammation in different tissue layers

Cooperation:
Department of Medicine B
University of Muenster

P. Lenz et al., Int. Biol. 5, 624-630 (2013), D. Bettenworth, et al., Histopathol. 33, 417-432 (2018).

Quantification of inflammation induced stenotic tissue alterations in unstained tissue

BIOMED TECH
BioMedizinisches Technologiezentrum

Surgical resection from Crohn's disease patients

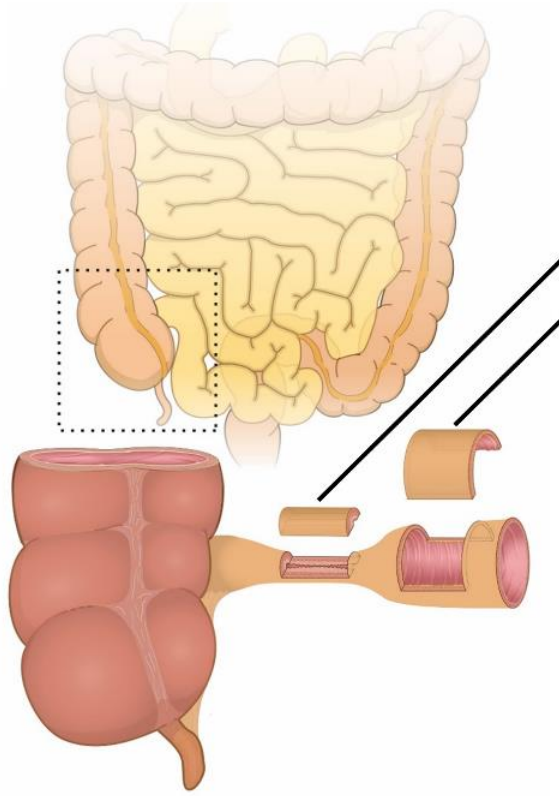

DHM QPI setup

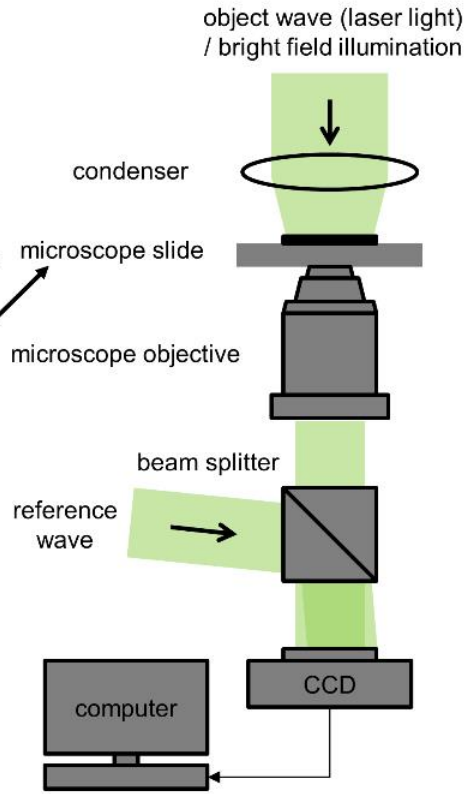

Representative stenotic tissue

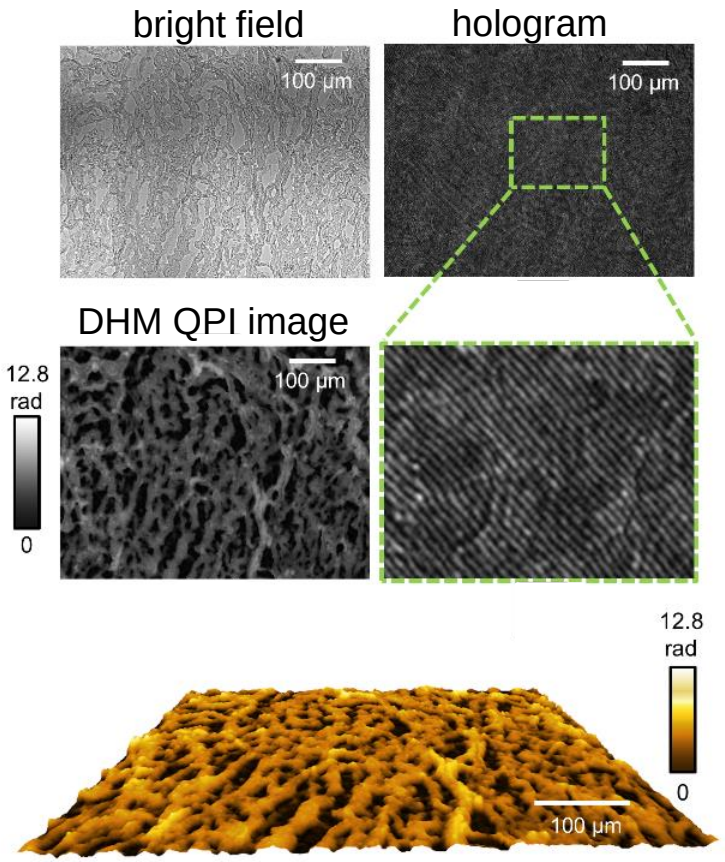

off-axis carrier fringes

pseudo 3D representation

A. Bokemeyer, et. al., Sci. Rep. 9, 19388 (2019).

Refractive index of stenotic tissue correlates with elasticity properties

26 surgical resection specimens from 13 Crohn's disease patients (stenosis vs. control)

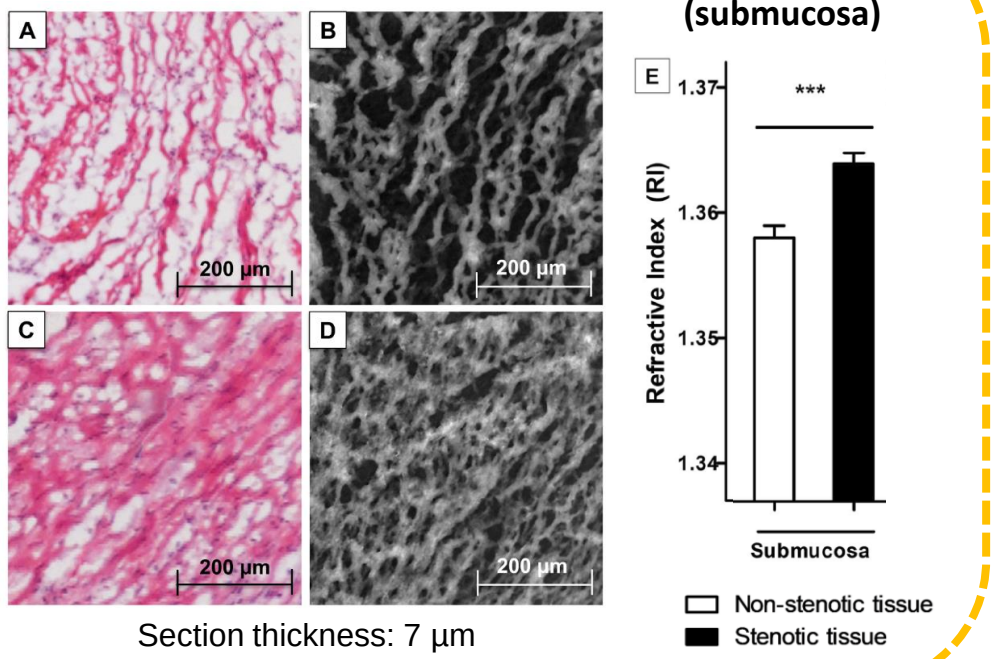

Section thickness: 7 µm

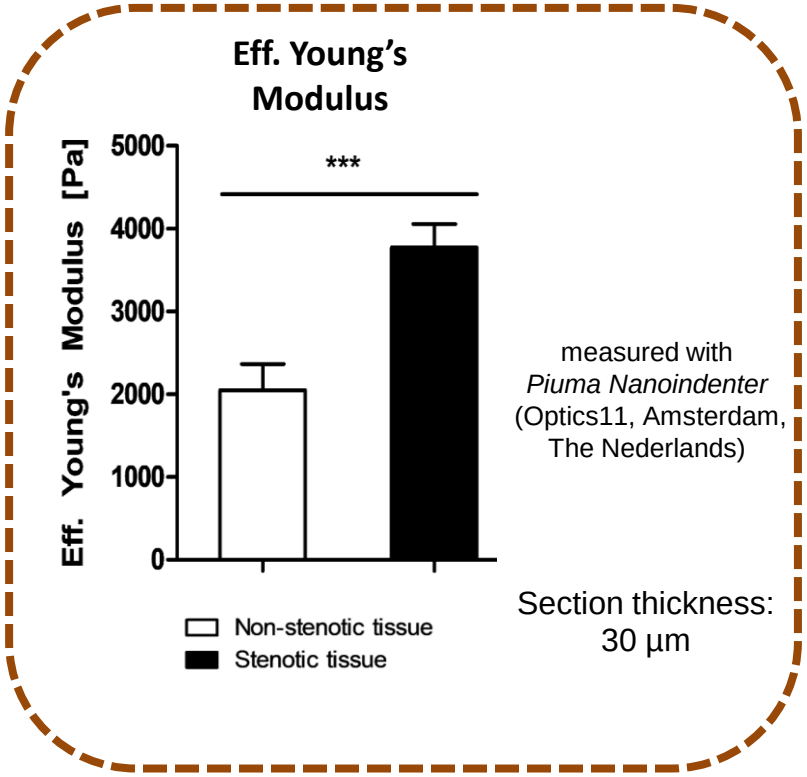

measured with *Piuma Nanoindenter* (Optics11, Amsterdam, The Nederlands)

Section thickness: 30 µm

***p<0.001

stenotic tissue ➔ significant higher stiffness
➔ **tissue refractive index reflects stiffness data retrieved by DHM**

A. Bokemeyer, et. al., Sci. Rep. 9, 19388 (2019).

Towards enhanced QPI image evaluation

BIOMED TECH
BioMedizinisches Technologiezentrum

Example: Automated detection of macrophages in quantitative phase images by deep learning using a Mask Region-based Convolutional Neural Network

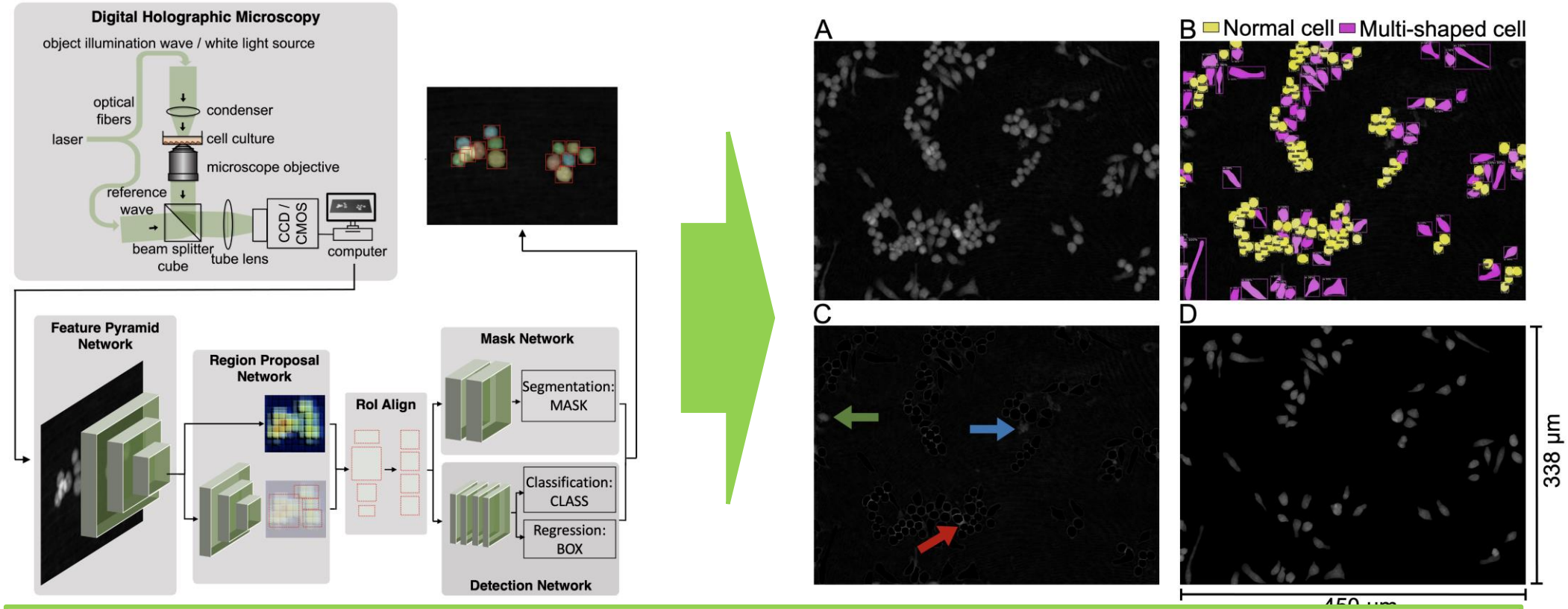

Mask R-CNN deep learning architecture ➔ simultaneous detection, segmentation and classification of RAW 264.7 mouse macrophages
(detection accuracy 93.5%)

K. Eder, T. Kutscher, et al., Proc. SPIE, 116551, 116551K (2021).

Conclusions

Quantitative phase imaging with DHM can address various topics in cell and tissue analysis by label-free quantification of:

- **motility** (automated migration trajectories, maximum migration distance, mean squared displacement,…)
- **growth / proliferation** (dry mass, area covered by cells, imaging of cell division events, cell counting)
- **morphology** (cell thickness/volume, tissue density/refractive index distribution)

by absolute biophysical parameters.

Future challenges

- accelerated procedures for image acquisition and data extraction
- achieving a statistically convincing amount of measurement data with minimized efforts and time
- enhanced specificity

}

- **robust laboratory systems**
- **simplified handling**
- **automation**
- **machine learning / AI assisted analysis**

⇒ **Multifunctional label-free tool for the analysis of cells *in-vitro* and *ex-vivo* tissues**

Selected references

Overview (very short):
B. Kemper, "Digital holographic microscopy enhances cytometry and histology", Europhotonics Winter 2019, 20-23 (2019).
https://www.photonics.com/Articles/Digital_Holographic_Microscopy_Enhances_Cytometry/a65240

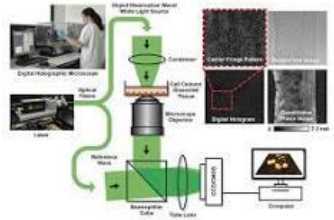

Overview live cell imaging (very long):
B. Kemper et al., Book Chapter "Label-free quantitative in-vitro live cell imaging with digital holographic microscopy", Bioanalytical Reviews (2019), Ed.: J. Wegener, BIOREV (2019) 2: 219–272 (Springer Nature Switzerland AG).

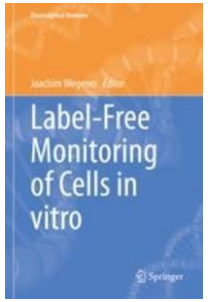

Overview dissected tissues:
D. Bettenworth, A. Bokemeier, C. Poremba, N. S. Ding, S. Ketelhut, P. Lenz, B. Kemper, "Quantitative phase microscopy for evaluation of intestinal inflammation and wound healing utilizing label-free biophysical markers" Review article, Histol. Histopathol. 33, 417-432 (2018).

More:
Google Scholar
Research gate

BIOMED
BioMedizinisches
Technologiezentrum
TECH

Thank you!

porcine intestine cells co-cultivated with Lactobacillus acidophilus